

# PRICING LEVERAGED ETFS OPTIONS UNDER HESTON DYNAMICS

A THESIS SUBMITTED TO AUCKLAND UNIVERSITY OF TECHNOLOGY  
IN PARTIAL FULFILMENT OF THE REQUIREMENTS FOR THE DEGREE OF  
MASTER OF SCIENCE

Supervisors

Prof. Jiling Cao

Dr. Wenjun Zhang

June 2018

By

Gaurav Kapoor

School of Engineering, Computer and Mathematical Sciences

# Copyright

Copyright in text of this thesis rests with the Author. Copies (by any process) either in full, or of extracts, may be made **only** in accordance with instructions given by the Author and lodged in the library, Auckland University of Technology. Details may be obtained from the Librarian. This page must form part of any such copies made. Further copies (by any process) of copies made in accordance with such instructions may not be made without the permission (in writing) of the Author.

The ownership of any intellectual property rights which may be described in this thesis is vested in the Auckland University of Technology, subject to any prior agreement to the contrary, and may not be made available for use by third parties without the written permission of the University, which will prescribe the terms and conditions of any such agreement.

Further information on the conditions under which disclosures and exploitation may take place is available from the Librarian.

© Copyright 2018. Gaurav Kapoor

# Declaration

I hereby declare that this submission is my own work and that, to the best of my knowledge and belief, it contains no material previously published or written by another person nor material which to a substantial extent has been accepted for the qualification of any other degree or diploma of a university or other institution of higher learning.

A handwritten signature in black ink that reads "G. Kapoor". The letters are cursive and fluid, with a large initial 'G' and a distinct dot over the 'i' in 'Kapoor'.

---

Signature of candidate

# Acknowledgements

Firstly, I would like to express my gratitude to my primary supervisor, Prof. Jiling Cao. Over the course of my studies, Prof. Cao has provided a solid foundation for my research without which this thesis would not be possible. His enthusiasm and sincerity was always a boost to my morale and I hope to redeem these qualities going forward. I would also like to thank my secondary supervisor, Dr. Wenjun Zhang. Wenjun provided valuable insight for my work in a friendly and genuine manner for which I am most grateful.

I would like to convey special thanks to Dr. Xinfeng Ruan. Xinfeng showed great sincerity in providing help and I am deeply grateful for that. He was always willing to offer advice and his dedication to acquire and share knowledge is a source of inspiration for me. I would also like to thank the rest of the AUT Financial Mathematics and Computation (AUT-FMC) Research Group. Our weekly thought-provoking discussions were incredibly helpful for my research and also outside of my academic work.

Throughout this journey, my family has provided me with continuous support and words of encouragement, for which I am extremely grateful. Their positivity has been a great motivator for me. Thanks to my friends outside academia who have always been supportive and understanding. Finally, I would like to thank Auckland University of Technology for all the opportunities I have been given time and again.

# Abstract

The aim of this thesis is to derive a pricing formula for options on leverage exchange-traded funds (LETFS) with the assumption that the underlying index follows the Heston model dynamics. In order to price options for LETFS, we first establish a relationship between the price of an LETF and the value of its underlying index. This relationship is dependent on the leverage ratio of the LETF and the volatility of the underlying index. Through empirical analysis, we are able to justify the accuracy of this link between an LETF and its underlying index. Furthermore, this link provides useful information on the behaviour of LETFS which is studied in depth. We also use an optimization technique to provide empirically estimated leverage ratios for various LETFS of VIX and several equities to understand their behaviour under different market conditions.

The option pricing formula is derived by defining the joint moment-generating function of the underlying index and its volatility and linking this function to the characteristic function of an LETF. The Carr-Madan Fourier transform method is utilized to obtain a closed-form solution of option prices in the form of an integral. We then numerically calculate the call option prices for specific parameters. We perform extensive analysis on our model. The call prices calculated from our option pricing formula are compared with those obtained by Monte-Carlo simulations and the results are consistent, justifying the use of our model. Finally, we perform sensitivity analysis to analyze the effect of various parametric changes on our model.

# Contents

<b>Copyright</b>	<b>ii</b>
<b>Declaration</b>	<b>iii</b>
<b>Acknowledgements</b>	<b>iv</b>
<b>Abstract</b>	<b>v</b>
<b>1 Introduction</b>	<b>1</b>
1.1 Introduction to Exchange-Traded Funds . . . . .	1
1.2 Introduction to Leveraged Exchange-Traded Funds . . . . .	2
1.3 Research Questions . . . . .	5
1.4 Contributions . . . . .	5
1.5 Research Ouputs . . . . .	7
<b>2 Mathematical Preliminaries</b>	<b>8</b>
2.1 Probability Theory . . . . .	8
2.1.1 Expectations and Conditional Expectations . . . . .	11
2.1.2 Moment Generating Functions . . . . .	13
2.1.3 Characteristic Functions . . . . .	14
2.2 Fourier Transform . . . . .	15
2.3 Stochastic Calculus . . . . .	17
2.3.1 Stochastic Processes . . . . .	17
2.3.2 Martingales and Markov Processes . . . . .	17
2.3.3 Brownian Motion . . . . .	19
2.3.4 Itô's Lemma . . . . .	20
2.3.5 Discounted Feynman-Kac Theorem . . . . .	21
<b>3 Price Dynamics of LETFs</b>	<b>24</b>
3.1 Modelling Returns of Leveraged ETFs . . . . .	24
3.1.1 Continuous-Time Model . . . . .	29
3.1.2 Empirical Validation . . . . .	31
3.2 Empirical Leverage Ratio Analysis . . . . .	35

<b>4</b>	<b>LETFs Option Pricing</b>	<b>43</b>
4.1	Heston Stochastic Volatility Model . . . . .	43
4.2	Derivation and Solution of Pricing PDE . . . . .	45
4.3	Option Pricing . . . . .	52
4.3.1	LETF Characteristic Function . . . . .	52
4.3.2	Carr-Madan Fourier Transform Method . . . . .	54
<b>5</b>	<b>Numerical Analysis</b>	<b>58</b>
5.1	Analysis of Option Pricing Formula . . . . .	59
5.1.1	Varying Time-to-Maturity . . . . .	63
5.1.2	Varying Moneyness . . . . .	67
5.2	Sensitivity Analysis . . . . .	68
5.2.1	Long-Run Variance Mean $\theta$ . . . . .	69
5.2.2	Initial Variance $v_0$ . . . . .	70
5.2.3	Variance Mean Reversion Rate $\kappa$ . . . . .	72
5.2.4	Volatility of Variance $\sigma$ . . . . .	73
5.2.5	Stock Price and Variance Correlation $\rho$ . . . . .	75
<b>6</b>	<b>Conclusion and Future Research</b>	<b>78</b>
	<b>References</b>	<b>81</b>
	<b>Appendix</b>	<b>82</b>

# List of Tables

3.1	Daily rebalancing of LETFs. . . . .	25
3.2	Data description. . . . .	32
3.3	Tracking error (%) of theoretical and empirical LETF returns. . . . .	34
3.4	Empirical $\beta$ estimates from optimization ( $\beta_{cub}$ ) and regression ( $\beta_{reg}$ ) methods. . . . .	39
3.5	Comparison of empirical $\beta$ estimates during positive and negative return periods. . . . .	41
5.1	Parameter values used to generate call option prices. . . . .	60
5.2	ATM call option prices from model and Monte Carlo simulations with 1,000, 10,000 and 100,000 paths. . . . .	62
5.3	Call prices generated from model and Monte Carlo simulations for various time-to-maturity levels. . . . .	65
5.4	Call prices generated from model and Monte Carlo simulations for various moneyness levels. . . . .	68

# List of Figures

3.1	Cumulative log-return of SPVXSTR (blue) and SVXY (red). . . . .	26
3.2	Empirical and theoretical returns comparison for various holding periods of $\pm 2x$ LETFs. . . . .	27
3.3	Empirical and theoretical returns comparison for various holding periods of $\pm 3x$ LETFs. . . . .	28
3.4	Correlation in log-returns of SPY and the $\pm 2x$ and $\pm 3x$ LETFs with their respective theoretical values. . . . .	33
3.5	Visual representation of estimation errors of $\beta_{cub}$ and $\beta_{reg}$ . . . . .	39
3.6	Visual representation of estimation errors of $\beta_{cub}^+$ and $\beta_{cub}^-$ . . . . .	41
5.1	Three sample paths of an LETF with $\beta = 2$ generated using Monte Carlo Simulations for 1000 trading days. . . . .	61
5.2	Three sample paths of an LETF with $\beta = 3$ generated using Monte Carlo Simulations for 1000 trading days. . . . .	62
5.3	Comparison of error between $Call_{Model}$ and $Call_{MC}$ with varying time-to-maturity. . . . .	64
5.4	Change in computational time and $\eta$ with time-to-maturity. . . . .	66
5.5	Comparison of error between $Call_{Model}$ and $Call_{MC}$ with varying money-ness. . . . .	69
5.6	Sensitivity of call option prices with $\theta$ . . . . .	70
5.7	Rate of change of call option prices with $\theta$ . . . . .	71
5.8	Sensitivity of call option prices with $v_0$ . . . . .	71
5.9	Rate of change of call option prices with $v_0$ . . . . .	72
5.10	Sensitivity of call option prices with $\kappa$ . . . . .	73
5.11	Rate of change of call option prices with $\kappa$ . . . . .	74
5.12	Sensitivity of call option prices with $\sigma$ . . . . .	74
5.13	Rate of change of call option prices with $\sigma$ . . . . .	75
5.14	Sensitivity of call option prices with $\rho$ . . . . .	76
5.15	Rate of change of call option prices with $\rho$ . . . . .	77

# Chapter 1

## Introduction

### 1.1 Introduction to Exchange-Traded Funds

An exchange-traded fund (ETF) is a type of investment fund, but unlike other index funds or mutual funds, its purpose is to track a specific index, such as a stock index, bond or commodity index. ETFs are traded on a public stock exchange similar to a common stock. An ETF trades roughly at the same price as the net value of the asset in its portfolio but its price may vary throughout the day as it is bought and sold.

ETFs are regulated by authorized participants (APs) who are market participants with a high degree of buying power, such as large financial institutions, banks or investment companies. APs interact with ETF providers in the process of creation or redemption of ETF shares. During creation, the APs make a portfolio of the underlying index and hand it over to the ETF providers in exchange for new ETF shares. Similarly, redemptions occur when APs return ETF shares to the providers in exchange for the basket of underlying assets. APs use this exchange to ensure that the intra-day ETF market prices are similar to the net values of the underlying asset.

ETFs were introduced to the US in 1993 and to Europe in 1996 and are extremely popular among individual investors, generating a large amount of volume daily. Two

notable ETFs are SPY, which tracks the S&P 500 Index, and the DIA, which tracks the Dow Jones Industrial Average. Equity ETFs make the largest contributions to assets under management with \$1.3 trillion worth of assets. The popularity of ETFs is largely due to higher daily liquidity and lower expense fees than mutual funds. Some other advantages are its ease of access, being able to sell short, the ability to buy on margin and having no minimum deposit amount, allowing the purchase of as low as one share.

## **1.2 Introduction to Leveraged Exchange-Traded Funds**

A leveraged exchange-traded fund (LETF) is simply an ETF which is designed to provide an amplified return of the underlying index it is tracking. The purpose of LETFs is to provide investors with the opportunity to catch short-term momentum bursts in its underlying index. The high risk that LETFs carry make them unattractive as long-term investments and traders are likely to hold them for a few days or less. The leverage ratio is the approximate ratio of returns the LETF attempts to achieve with respect to its underlying index. An LETF can be both bullish, which provides a positive ratio in returns, commonly 2 or 3 times the daily index return, or bearish, which provides negative returns, commonly -1, -2 or -3 times the daily index return. Bearish LETFs are a popular alternative to short-selling of assets, as they usually have lower expense fees. Since an ordinary ETF tracks the exact returns of an index, it is considered to be passively managed, whereas an LETF undergoes daily rebalancing in the form of borrowing funds to purchase additional shares, or short-selling in the case of bearish LETFs.

Since their introduction, LETFs have drawn a number of criticisms regarding their ability to provide the returns they should, especially during financial crises when volatility is at its peak. LETFs are known to under-perform over longer time horizons and will usually fall short of their advertised leverage ratio. The daily rebalancing

mechanism means that despite having accurate returns on a daily basis, LETFs will slowly diminish in performance as the variance of their underlying index is compounded over time. This under-performance is also often a result of poorly timed rebalancing and the replication of returns through derivatives.

Cheng and Madhavan in [7] illustrated the behaviour of LETF prices with respect to the variance of their underlying index. They showed the variation in the desired and actual returns of an LETF over a long time period was a consequence of its daily rebalancing as well as the strong dependence of an LETF on the variance of its underlying index. This erosion of LETF prices can lead to a bullish LETF having negative returns when its underlying index has positive returns, or a bearish LETF having losses when its underlying index returns is also having losses. In August 2009, the US Securities and Exchange Commission issued a statement regarding the riskiness of LETFs and investigated a potential feedback loop created by LETFs which could lead to higher market volatility. Lu, Wang and Zhang in [17] created a discrete-time model showing the long-term performance of LETFs. This relationship was also modeled by Avellaneda and Zhang [4] with a continuous-time model. Leung and Santoli [14] and Mason et al. [18] showed the empirical leverage ratios of certain LETFs and discussed certain portfolio rebalancing techniques to reduce errors in returns and also illustrated certain investment strategies for LETFs using these techniques.

The concept of options on LETFs is fairly new and so the research done is limited. Zhang in [23] stated that the relationship between an LETF and its underlying index is "path-dependent" and proposed a Heston model framework for options pricing which was applied to various LETFs tracking the S&P 500 Index. The results showed that an LETF option can be replicated through a basket of options on the underlying index with a suitable choice of strike prices. These derivations were influenced by the path-dependence ideology. The theory was tested empirically and showed a strong correlation with actual mid-market prices. The findings of Zhang were extended by Ahn et al. [1]

and applied to the stochastic volatility with jump (SVJ) and the stochastic volatility with contemporaneous jump (SVCJ) models. They also used the Heston model and showed that if the underlying index has Heston dynamics, then so does the LETF. They applied standard transform methods to analytically price both ETFs and LETFs. In the case that a closed-form expression could not be computed, they discussed some numerical solutions and approximation methods as proposed by Heston [13].

Since LETFs not only share an underlying index but also the same sources of risk, the value of these LETFs should have a strong relationship. Therefore it is of theoretical and practical importance to implement an option pricing framework that is arbitrage-free and compatible amongst different leverage ratios. Alexander and Kaeck [3] found better results when modeling the log-value of the VIX and so they proposed a stochastic volatility model for the log of VIX for pricing options. Leung and Santoli in [14] proposed a Heston stochastic volatility model with jumps for the underlying index due its tractability and ability to recreate similar volatility characteristics for different LETFs. Ahn et al. [1] introduced an approximate pricing method to price LETF options consistently for various jump-diffusion model. They also explore the impact of daily rebalancing frequency on the price of an LETF option. This effect was also noted by Santoli [20]. Deng et al. [10] compared empirical LETF implied volatilities with implied volatilities simulated from the Heston model. Gehricke and Zhang [11] were particularly interested in the VXX, and they proposed a model focusing on the time-varying mean behavior of the VXX. Leung and Sircar [16] used asymptotic techniques to derive approximations for LETF option prices and its implied volatility under a stochastic volatility framework. Most recently, Xu [22] discussed several jump-diffusion models, separating equity and volatility LETFs. Using the Fast Fourier Transform (FFT) method introduced by Carr and Madan [6], a consistent framework was developed to obtain a closed-form options pricing formula. The volatility models had particular interest in the VIX and its ETFs. Xu did not account for the path-dependence

of LETFs in their model. Furthermore, no numerical analysis was performed to justify their model's ability to provide accurate option prices. In our thesis, we extend the research of Xu [22] and implement the path-dependence of LETFs into our model and provide numerical results with comparisons to Monte-Carlo simulated call prices.

### 1.3 Research Questions

The contribution of this thesis can be summarized as the pursuit to answer the following research questions.

**Question 1.1.** *Can the optimization technique for estimating empirical leverage ratios, introduced in [15], provide better estimates over traditional methods in different market conditions?*

**Question 1.2.** *How can we create a consistent framework for pricing LETF options that incorporates its path-dependent property?*

**Question 1.3.** *How are the call option prices obtained from our formula affected by changes in the underlying model parameters? Will our model be able to provide accurate results under extreme parametric conditions?*

### 1.4 Contributions

Chapter 3 of this thesis presents the mathematical framework of LETFs. In this chapter, we model the relationship between the price of an LETF and the value of its underlying index and attempt to explain key characteristics of LETFs using this link. The relationship shows the dependence of an LETF's price on not only the value of its underlying index, but also the LETF's leverage ratio and the volatility of the underlying index. The volatility coefficient in this model, which is a function of the leverage ratio, is shown to be negative for any leverage ratio. This explains the volatility decay characteristic

of an ETF which is a large cause of concern amongst investors. The volatility decay factor accumulates over time and will have significant negative impact on the returns of ETFs over longer time horizons. This accumulated volatility over time also leads to the path-dependence of ETFs.

We use an optimization technique, introduced by Leung and Santoli in [15], to empirically estimate the leverage ratio of an ETF under different market conditions and with varying holding period lengths. Results from the optimization method are compared to those from standard regression analysis, and the optimization method shows lower errors between the estimated and theoretical leverage ratio values. While this does not necessarily suggest that the optimization technique produces better results, there are several drawbacks of using the regression method which makes the optimization method a credible alternative. The results from our analysis show that longer holding periods lead to severe under-performance of ETFs due to the volatility decay factor, as mentioned previously. In bullish markets, the bullish ETFs perform better on average and bearish ETFs perform slightly worse. In bearish markets, both types of ETFs perform significantly worse. This conclusion is logical since bearish markets are generally associated with higher volatility, which in turn leads to larger volatility decay in ETFs and overall worse performance.

Chapter 4 of this thesis provides the option pricing methodology. The underlying index of an ETF is modeled under Heston dynamics. Another process is introduced here to exhibit the path-dependent property of ETFs. Using the joint moment generating function (MGF) of the underlying index value and its volatility, we are able to derive a pricing PDE. The joint MGF is assumed to follow an exponential affine form, and we are able to obtain a closed-form solution to the PDE. We establish a link between the joint MGF and the characteristic function of an ETF. Finally, we use the Carr-Madan Fourier transform method to derive our option pricing formula in the form of an integral. Our submitted research paper [5] highlights the crucial parts of

this option pricing methodology and further extends this procedure by applying the fast Fourier transform. More details on this paper are provided in Section 1.4.

Chapter 5 of this thesis presents the numerical analysis of our option pricing model by comparing the call prices obtained using our formula to the theoretical prices from Monte Carlo simulations. The results show very low error between our model and simulations and justifies the accuracy of our option pricing model. This chapter also analyses the sensitivity in call prices with respect to the Heston model parameters. The sensitivity analysis provides a necessary understanding of LETF option prices under various market conditions and also shows the durability of our model to be able to provide accurate results under extreme parametric conditions.

## 1.5 Research Ouputs

During the course of this Master's thesis, the following research paper was completed.

[A] Cao, J., Kapoor, G., Ruan, X., Zhang, W. (2018). Path-dependent leveraged exchange-traded fund option pricing using the fast fourier transform. Submitted to *Computers and Mathematics with Applications*, Elsevier.

The LETF option pricing methodology introduced in this thesis is explained concisely in the paper [A]. This paper extends the research of this thesis by applying the fast Fourier transform to our call price integral.

# Chapter 2

## Mathematical Preliminaries

In this chapter, we introduce some mathematical preliminaries and techniques that are applied in our thesis. The majority of the material used in this chapter is taken from textbooks [8], [19] and [21].

### 2.1 Probability Theory

A probability space is defined as a triple,  $(\Omega, \mathcal{F}, \mathbb{P})$ . Here,  $\Omega$  is a space of possible outcomes,  $\mathcal{F}$  is a  $\sigma$ -algebra on  $\Omega$ , and  $\mathbb{P}$  is a probability measure.

**Definition 2.1.1.** ( $\sigma$ -algebra). A non-empty collection  $\mathcal{F}$  of subsets of  $\Omega$  is called a  $\sigma$ -algebra on  $\Omega$  if and only if

- (i) the null set  $\emptyset \in \mathcal{F}$ ,
- (ii)  $A \in \mathcal{F} \Rightarrow A^c \in \mathcal{F}$ , where  $A^c$  denotes the complement of  $A$  in  $\Omega$ ,
- (iii) the union of a countable collection of sets in  $\mathcal{F}$  is also in  $\mathcal{F}$ , i.e. if  $A_1, A_2, \dots$  are in  $\mathcal{F}$ , then  $\bigcup_{n \geq 1} A_n \in \mathcal{F}$ .

As a result,  $\Omega \in \mathcal{F}$ . The pair  $(\Omega, \mathcal{F})$  is called a measurable space. A probability measure  $\mathbb{P}$  on a measurable space  $(\Omega, \mathcal{F})$  is a nonnegative set function defined on  $\mathcal{F}$  that

satisfies (i)  $\mathbb{P}(\Omega) = 1$  and (ii) for any sequence of pairwise disjoint sets  $A_1, A_2, \dots, A_n$ ,

$$\mathbb{P}\left(\bigcup_{i=1}^{\infty} A_i\right) = \sum_{i=1}^{\infty} \mathbb{P}(A_i). \quad (2.1)$$

To summarize, a probability space  $(\Omega, \mathcal{F}, \mathbb{P})$  is a measurable space  $(\Omega, \mathcal{F})$  together with a probability measure  $\mathbb{P}$  defined on  $\mathcal{F}$ .  $\Omega$  alone is called a sample space, and each of its elements, denoted  $\omega$ , is a sample point, every member of  $\mathcal{F}$  is an event, and  $\mathbb{P}$  is the probability measure.

**Definition 2.1.2.** (Random Variables). Let  $(\Omega, \mathcal{F}, \mathbb{P})$  denote a probability space. Then a *random variable*, denoted  $X$ , is a real-valued function defined on the sample space  $\Omega$  if it satisfies the property that for every Borel subset  $B$  of  $\mathbb{R}$ , the subset of  $\Omega$  given by

$$X^{-1}(B) = \{\omega \in \Omega : X(\omega) \in B\}. \quad (2.2)$$

is in  $\mathcal{F}$ .

For a better understanding of Definition 2.1.2, we must define the Borel subsets of  $\mathbb{R}$ . To define the Borel subsets of  $\mathbb{R}$ , we first consider the closed intervals  $[a, b] \subset \mathbb{R}$  and then proceed to add all possible sets that are necessary to have a  $\sigma$ -algebra. Therefore, all possible unions of sequences of closed intervals are Borel sets. Since every open interval can be defined as a union of sequence of closed intervals, an open interval is also a Borel set. Furthermore, a union of sequences of open intervals can form an open set, where an interval may or may not be defined, and so an open set is also a Borel set. Also, the complement of an open set, a closed set, is also a Borel set. This collection of Borel subsets in  $\mathbb{R}$  is called the Borel  $\sigma$ -algebra of  $\mathbb{R}$  and every subset of  $\mathbb{R}$  encountered henceforth is within the Borel  $\sigma$ -algebra.

A random variable  $X$  is then a numerical value determined through an experiment of choosing  $\omega \in \Omega$ , i.e, the value obtained as a result of a specific outcome within the

set of all possible outcomes. Furthermore, it is of interest to understand the probability of  $X$  taking on each outcome. Since, in most cases, the probability of a single outcome occurring is 0, it is better to consider the outcome within a certain Borel set, i.e.,  $\mathbb{P}\{X \in B\}$ , where  $B$  is a Borel subset. With this in mind, the probability distribution of  $X$  can then be defined.

**Definition 2.1.3.** (Distribution Measure). Let  $(\Omega, \mathcal{F}, \mathbb{P})$  denote a probability space and  $X$  is a random variable on this space. The *distribution measure* of  $X$  is defined as a probability measure  $\mu_X$  which is assigned to each Borel subset  $B$ , where  $\mu_X(B)$  denotes the probability of  $X$  being a value within this subset, i.e.,  $\mu_X(B) = \mathbb{P}\{X \in B\}$ .

Pricing financial derivatives by applying knowledge of the no-arbitrage pricing theory requires a contingency plan. The contingency plan accounts for the initial wealth necessary to set up a hedging short position which is contingent on the uncertainty between the present and future time. For continuous-time models, we must create a sophisticated process to understand the concept of information about an asset at a given time.

We can express the concept of information in terms of  $\sigma$ -algebras from Definition 2.1.1. A  $\sigma$ -algebra is a collection of subsets of the sample space  $\Omega$ , i.e., it is a representation of all possible outcomes of an experiment at a given time. A  $\sigma$ -algebra can be thought of as the information received about that experiment at a given time. Using the  $\sigma$ -algebra containing all possible outcomes from the current time, we can express the  $\sigma$ -algebra of a future time and all its possible outcomes, which includes the outcomes from the previous  $\sigma$ -algebra. In this manner, we construct a collection of  $\sigma$ -algebras which provides more information over time. This collection of  $\sigma$ -algebras is called a filtration.

**Definition 2.1.4.** (Filtration). Consider a probability space  $(\Omega, \mathcal{F}, \mathbb{P})$ . Let  $T > 0$  and assume that for every  $t \in [0, T]$  there is a  $\sigma$ -algebra  $\mathcal{F}(t)$ . Let  $s$  represent a time where

$s \leq t$ , and every set within  $\mathcal{F}(s)$  is also in  $\mathcal{F}(t)$ . Then, the collection of  $\sigma$ -algebras  $\mathcal{F}(t)$ ,  $0 \leq t \leq T$ , is called a *filtration*.

**Definition 2.1.5.** Consider a probability space  $(\Omega, \mathcal{F}, \mathbb{P})$  and a random variable  $X$  defined on  $(\Omega, \mathcal{F}, \mathbb{P})$ . The  $\sigma$ -algebra generated by  $X$ , denoted by  $\sigma(X)$ , is a collection of all sets of the form  $X^{-1}(B)$  where  $B$  is a Borel set of  $\mathbb{R}$ .

**Definition 2.1.6.** Consider a probability space  $(\Omega, \mathcal{F}, \mathbb{P})$  and a random variable  $X$  defined on  $(\Omega, \mathcal{F}, \mathbb{P})$ . Denote  $\mathcal{G}$  a  $\sigma$ -algebra of subsets of  $\Omega$ . Then if every set within  $\sigma(X)$  is also in  $\mathcal{G}$ , we say that  $X$  is  $\mathcal{G}$ -measurable.

Note that, if  $X$  is  $\mathcal{G}$ -measurable, then  $f(X)$  is also  $\mathcal{G}$ -measurable, where  $f : \mathbb{R} \rightarrow \mathbb{R}$  is any Borel-measurable function. If  $\mathcal{G}$  is able to ascertain the value of  $X$  then it can also do so for  $f(X)$ .

### 2.1.1 Expectations and Conditional Expectations

Consider a probability space  $(\Omega, \mathcal{F}, \mathbb{P})$  and a random variable  $X$  defined on  $(\Omega, \mathcal{F}, \mathbb{P})$ . The mathematical expectation of  $X$ , denoted by  $\mathbb{E}[X]$ , is defined as

$$\mathbb{E}[X] = \int_{\Omega} X d\mathbb{P} = \int_{\mathbb{R}} xf(x)dx, \quad (2.3)$$

where  $f(x)$  is the probability density function of  $X$ .

Consider a probability space  $(\Omega, \mathcal{F}, \mathbb{P})$ , a random variable  $X$  defined on this space and a sub- $\sigma$ -algebra  $\mathcal{G}$  of  $\mathcal{F}$ . If  $X$  is  $\mathcal{G}$ -measurable, then the information from  $\mathcal{G}$  is sufficient to determine the value of  $X$ . On the other hand, if  $\mathcal{G}$  is independent of  $X$ , then the information from  $\mathcal{G}$  is of no use. In the median case, the information from  $\mathcal{G}$  is able to provide a reasonable estimate for the value of  $X$ . In this case, we can say that the estimate of  $X$  is conditional on the information from  $\mathcal{G}$ . In other words, the conditional expectation of  $X$  given  $\mathcal{G}$  provides an estimate for the value of  $X$ .

**Definition 2.1.7.** Consider the probability space  $(\Omega, \mathcal{F}, \mathbb{P})$ , a random variable  $X$  defined on  $(\Omega, \mathcal{F}, \mathbb{P})$  and a sub- $\sigma$ -algebra  $\mathcal{G}$ , where  $\mathcal{G} \subseteq \mathcal{F}$ . The *conditional expectation* of  $X$  given  $\mathcal{G}$ , denoted by  $\mathbb{E}[X|\mathcal{G}]$ , is a random variable that satisfies

- (i) **(Measurability)**  $\mathbb{E}[X|\mathcal{G}]$  is  $\mathcal{G}$ -measurable, and
- (ii) **(Partial averaging)**

$$\int_A \mathbb{E}[X|\mathcal{G}](\omega) d\mathbb{P}(\omega) = \int_A X(\omega) d\mathbb{P}(\omega) \quad \text{for all } A \in \mathcal{G}. \quad (2.4)$$

The first property from Definition 2.1.7 ensures that the value of conditional expectation can be ascertained from the information in  $\mathcal{G}$ . The second property guarantees that  $\mathbb{E}[X|\mathcal{G}]$  is an estimate of  $X$ . Note that if the  $\sigma$ -algebra  $\mathcal{G}$  is generated from another random variable  $G$ , then the conditional expectation would generally be written in terms of  $G$ , i.e.,  $\mathbb{E}[X|G]$  rather than  $\mathbb{E}[X|\mathcal{G}]$ . Also, there will always exist a unique random variable that satisfies both properties (i) and (ii).

The following proposition summarizes some fundamental properties of conditional expectations.

**Proposition 2.1.1.** Consider the probability space  $(\Omega, \mathcal{F}, \mathbb{P})$  and denote  $\mathcal{G}$  a sub- $\sigma$ -algebra of  $\mathcal{F}$ .

- (i) **(Linearity)** Let  $X$  and  $Y$  denote integrable random variables, and  $c_1$  and  $c_2$  are constants, then

$$\mathbb{E}[c_1X + c_2Y|\mathcal{G}] = c_1\mathbb{E}[X|\mathcal{G}] + c_2\mathbb{E}[Y|\mathcal{G}]. \quad (2.5)$$

- (ii) **(Taking out known factor)** Let  $X$  and  $Y$  denote integrable random variables,

and  $X$  is  $\mathcal{G}$ -measurable, then

$$\mathbb{E}[XY|\mathcal{G}] = X\mathbb{E}[Y|\mathcal{G}]. \quad (2.6)$$

(iii) (**Tower property**) Let  $X$  denote an integrable random variable, and  $\mathcal{H}$  is a sub- $\sigma$ -algebra of  $\mathcal{G}$ , i.e,  $\mathcal{H}$  contains less information than  $\mathcal{G}$ , then

$$\mathbb{E}[\mathbb{E}[X|\mathcal{G}]|\mathcal{H}] = \mathbb{E}[X|\mathcal{H}]. \quad (2.7)$$

(iv) (**Independence**) Let  $X$  denote an integrable random variable that is independent of  $\sigma$ -algebra  $\mathcal{G}$ , then

$$\mathbb{E}[X|\mathcal{G}] = \mathbb{E}[X]. \quad (2.8)$$

### 2.1.2 Moment Generating Functions

In probability theory, the moment generating function (MGF) of a random variable is another way to define its probability distribution. Its applications to options pricing theory allow for another method to analytically derive an option pricing formula. Note that the MGF of a random variable may not always exist.

**Definition 2.1.8.** Let  $X$  denote a real-valued random variable, then its *moment generating function*  $M_X(u)$  is defined as

$$M_X(u) = \mathbb{E}[e^{uX}], \quad (2.9)$$

wherever this expectation may exist, and where  $u \in \mathbb{R}$ . Note that  $M_X(0)$  always exists and is equal to 1. The MGF can also be written in terms of the probability density

function  $f_X(x)$  of  $X$  as

$$M_X(u) = \int_{-\infty}^{\infty} e^{ux} f_X(x) dx. \quad (2.10)$$

**Definition 2.1.9.** Consider an  $n$ -dimensional vector of random variables  $\mathbf{X} = (X_1, \dots, X_n)^T$  and an  $n$ -dimensional fixed vector  $\mathbf{u}$ , then the *joint moment generating function* of  $\mathbf{X}$  is

$$M_{\mathbf{X}}(\mathbf{u}) = \mathbb{E} \left[ e^{\mathbf{u}^T \mathbf{X}} \right], \quad (2.11)$$

where  $\mathbf{u}^T$  denotes the transpose of  $\mathbf{u}$ .

### 2.1.3 Characteristic Functions

The characteristic function (CF) of a random variable  $X$ , denoted by  $\phi_X(u)$ , is closely related to its MGF,  $M_X(u)$ . The CF is defined as the MGF of  $iX$ , i.e, it is evaluated on the imaginary axis. The CF is able to completely define the probability distribution of a random variable, and unlike the MGF, it always exists, even if the probability density function does not.

**Definition 2.1.10.** Let  $X$  denote a real-valued random variable, then its *characteristic function*  $\phi_X(u)$  is defined as

$$\phi_X u = \mathbb{E} \left[ e^{iuX} \right], \quad (2.12)$$

where  $i = \sqrt{-1}$ . This definition suggests an immediate link between the MGF and CF

$$M_X(u) = \phi_X(-iu), \quad (2.13)$$

or in terms of the characteristic function

$$\phi_X(u) = M_X(iu). \quad (2.14)$$

Since there is a bijection between the CF and the cumulative distribution function of a random variable, it is always possible to obtain one of these functions from the other. Using an inversion theorem, the characteristic function can be linked to the probability density function (PDF) and cumulative distribution function (CDF) of a random variable.

**Proposition 2.1.2.** Consider a random variable  $X$  and let  $f_X(x)$ ,  $F_X(x)$  and  $\phi_X(u)$  denote its PDF, CDF and CF, respectively. Then the link between these functions is

$$f_X(x) = F'_X(x) = \frac{1}{2\pi} \int_{-\infty}^{\infty} e^{-iux} \phi_X(u) du, \quad (2.15)$$

where  $F'_X(x)$  denotes the derivate of  $F_X(x)$  with respect to  $x$ .

Proposition 2.1.2 is an application of the inverse Fourier transform which is discussed in the next section.

## 2.2 Fourier Transform

The Fourier transform has many applications in Mathematics. In Chapter 4 of this thesis, the Fourier transform and inverse Fourier transform methods are applied in an option pricing environment to derive a European call price function for LETFs. Using these methods, we are also able to establish a relationship between the PDF and CF of a random variable, as was shown in the previous section.

**Definition 2.2.1.** Let  $f(x)$  denote a function defined on  $\mathbb{R}$ . The *Fourier transform* of  $f$

is defined as

$$\mathfrak{F}(z) := \int_{-\infty}^{\infty} f(x)e^{-izx} dx, \quad (2.16)$$

where  $i = \sqrt{-1}$  and  $z$  represents the Fourier transform variable.

The operator  $\Phi : f \mapsto \mathfrak{F}$  is called the Fourier transform operator. In this case, we write

$$f(x) = \frac{1}{2\pi} \int_{-\infty}^{+\infty} \mathfrak{F}(z)e^{izx} dz, \quad (2.17)$$

and  $f = \Phi^{-1}(\mathfrak{F})$ , where  $\Phi^{-1}$  is called the inverse Fourier transform operator. We say that  $f(x)$  and  $\mathfrak{F}(z)$  form a Fourier transform pair.

Using these definitions, we can apply the Fourier transform methods to show the link between the CF and PDF of a random variable.

**Proposition 2.2.1.** Consider a random variable  $X$ , and let  $f_X(x)$  and  $\phi_X(u)$  denote its PDF and CF, respectively. Then the CF of  $X$  can be defined as the Fourier transform of its PDF

$$\phi_X(u) = \mathbb{E}[e^{iuX}] = \int_{-\infty}^{+\infty} e^{iuX} f_X(x) dx. \quad (2.18)$$

Through the inverse Fourier transform, we can obtain  $f_X(x)$  as in Proposition 2.1.2

$$f_X(x) = \frac{1}{2\pi} \int_{-\infty}^{+\infty} e^{-iux} \phi_X(u) du. \quad (2.19)$$

## 2.3 Stochastic Calculus

### 2.3.1 Stochastic Processes

In probability theory, a stochastic process is defined as a collection of random variables. This collection is indexed by a set of numbers, and in most cases this set corresponds to a time interval. If the index set has finite or a countable number of elements, we refer to the process as a discrete-time stochastic process. On the other hand, if the index set is an interval on the real line, we say that it is a continuous-time stochastic process.

**Definition 2.3.1.** A *stochastic process* is a collection of random variables defined on a probability space  $(\Omega, \mathcal{F}, \mathbb{P})$ . The random variables are indexed by a set  $T$ . When  $T$  is the set of natural numbers  $\mathbb{N}$ , we denote a discrete-time stochastic process as

$$\{X_n : n \in \mathbb{N}\}.$$

When  $T = [0, +\infty)$ , we denote a continuous-time stochastic process as

$$\{X_t : t \geq 0\}.$$

**Definition 2.3.2.** Consider a probability space  $(\Omega, \mathcal{F}, \mathbb{P})$  and an associated filtration  $\{\mathcal{F}_t : t \geq 0\}$ . Let  $\{X_t : t \geq 0\}$  denote a stochastic process. We would call  $\{X_t : t \geq 0\}$  an *adapted stochastic process* if, for each  $t$ ,  $X_t$  is  $\mathcal{F}_t$ -measurable.

### 2.3.2 Martingales and Markov Processes

Recall that a filtration on  $(\Omega, \mathcal{F}, \mathbb{P})$  is described as a non-decreasing family  $\{\mathcal{F}_t : t \geq 0\}$  of sub  $\sigma$ -algebras of  $\mathcal{F}$ , that is, for  $0 \leq s < t$

$$\mathcal{F}_s \subseteq \mathcal{F}_t \subseteq \mathcal{F}.$$

Then,  $(\Omega, \mathcal{F}, \mathbb{P}, \{\mathcal{F}_t : t \geq 0\})$  is called a filtered probability space.

**Definition 2.3.3.** A real-valued stochastic process  $\{X_t : t \geq 0\}$ , adapted to the filtration  $\{\mathcal{F}_t : t \geq 0\}$ , is a *martingale* relative to  $\{\mathcal{F}_t : t \geq 0\}$  if

- (i) for each  $t$ ,  $\mathbb{E}[X_t] < \infty$ , i.e.,  $X_t$  is integrable,
- (ii) for any pair  $s, t \in T$  where  $s \leq t$ ,  $\mathbb{E}[X_t | \mathcal{F}_s] = X_s$ .

The process  $\{X_t : t \geq 0\}$  is called a sub-martingale if  $\mathbb{E}[X_t | \mathcal{F}_s] \geq X_s$  within the same conditions. Similarly,  $\{X_t : t \geq 0\}$  is called a super-martingale if  $\mathbb{E}[X_t | \mathcal{F}_s] \leq X_s$ . Therefore, a process which is both a sub-martingale and a super-martingale is a martingale.

In probability theory, the Markov property is a term used to describe the memoryless property of a stochastic process. A stochastic process holds the Markov property if its future value depends only on the present value and is conditionally independent of all previous values. In other words, the past behavior of a stochastic process is of no use in predicting its future behavior given the current state of the process. A stochastic process that possesses this property is known as a Markov process.

**Definition 2.3.4.** Consider a probability space  $(\Omega, \mathcal{F}, \mathbb{P})$ , let  $T$  denote a fixed positive number and let  $\{\mathcal{F}_t : 0 \leq t \leq T\}$  be a filtration. Let  $\{X_t : 0 \leq t \leq T\}$  denote an adapted stochastic process. Assume that for all  $s$  and  $t$ , where  $s \leq t$ , and for every non-negative Borel-measurable function  $f$ , there exists another Borel-measurable function  $g$  such that

$$\mathbb{E}[f(X_t) | \mathcal{F}_s] = g(X_s). \quad (2.20)$$

Then we say that  $\{X_t : 0 \leq t \leq T\}$  is a *Markov process*.

### 2.3.3 Brownian Motion

**Definition 2.3.5.** Consider a probability space  $(\Omega, \mathcal{F}, \mathbb{P})$ . For each  $\omega \in \Omega$ , suppose there exists a continuous-time process  $\{B_t : t \geq 0\}$ . This process is called a *Brownian motion* if it satisfies the following properties

- (i) for all  $0 = t_0 < t_1 < \dots < t_n$ , the increments,

$$B_{t_1} - B_{t_0}, B_{t_2} - B_{t_1}, \dots, B_{t_n} - B_{t_{n-1}}$$

are independent, with  $B_0 = 0$ .

- (ii) for every  $s, t$ , where  $0 < s < t$ ,  $B_t - B_s$  follows a normal distribution with mean zero and variance  $t - s$ .

Brownian motion can also be defined relative to the filtration  $\{\mathcal{F}_t : t \geq 0\}$ .

**Definition 2.3.6.** Let  $(\Omega, \mathcal{F}, \mathbb{P})$  be a probability space on which a Brownian motion  $\{B_t : t \geq 0\}$  is defined. A *filtration* for  $B_t$  is a collection of  $\sigma$ -algebras  $\{\mathcal{F}_t : t \geq 0\}$  which satisfy

- (i) For every  $s, t$  where  $0 \leq s < t$ ,  $\mathcal{F}_s \subseteq \mathcal{F}_t$ . That is, the information available at a later time  $\mathcal{F}_t$  contains all information available at an earlier time  $\mathcal{F}_s$ .
- (ii) For every  $s, t$  where  $0 \leq s < t$ , the increment  $B_t - B_s$  is independent of  $\mathcal{F}_s$ . Essentially, the increments of Brownian motion after time  $s$  are independent of the information available up to time  $t$ .
- (iii) For each  $t \geq 0$  the Brownian motion  $B_t$  at time  $t$  is  $\mathcal{F}_t$ -measurable. Therefore, the information available at time  $t$  is sufficient to evaluate  $B_t$  at that time.

### Brownian Motion as Martingale

Let  $\{\mathcal{F}_t : t \geq 0\}$  denote a filtration for a Brownian motion  $\{B_t : t \geq 0\}$ . By definition,  $B_t$  follows a normal distribution with mean zero and variance  $t$ , and is therefore integrable with  $\mathbb{E}[B_t] = 0$ , thus satisfying Definition 2.3.3 (i). Property (ii) can be proven as follows. For any time  $0 \leq s < t$

$$\begin{aligned}\mathbb{E}[B_t | \mathcal{F}_s] &= \mathbb{E}[B_s + (B_t - B_s) | \mathcal{F}_s] \\ &= \mathbb{E}[B_s | \mathcal{F}_s] + \mathbb{E}[B_t - B_s | \mathcal{F}_s] \\ &= B_s + \mathbb{E}[B_t - B_s] = B_s.\end{aligned}$$

Therefore, Brownian motion is a martingale. The second equality of this proof follows from the independence of increments of Brownian motion property, and the third equality uses the stationary normal increments property, Definition 2.3.5 (i) and (ii), respectively.

### 2.3.4 Itô's Lemma

**Definition 2.3.7.** Consider a probability space  $(\Omega, \mathcal{F}, \mathbb{P})$ , let  $\{B_t : t \geq 0\}$  denote a Brownian motion process on  $(\Omega, \mathcal{F}, \mathbb{P})$  and let  $\{\mathcal{F}_t : t \geq 0\}$  be its associated filtration. An *Itô process*  $\{X_t : t \geq 0\}$ , is an adapted stochastic process of the form

$$X_t = X_0 + \int_0^t \mu(s, X_s) ds + \int_0^t \sigma(s, X_s) dB_s, \quad (2.21)$$

where  $X_0$  is defined, and  $\mu(s, X_s)$  and  $\sigma(s, X_s)$  are adapted stochastic processes.

**Definition 2.3.8.** The *Itô differential equation* stems from the definition of an Itô process

and satisfies the stochastic differential equation

$$dX_t = \mu(t, X_t)dt + \sigma(t, X_t)dB_t. \quad (2.22)$$

An important result of Itô processes is the derivation of Itô's lemma, which is used in stochastic calculus to find the differential of a time-dependent function.

**Proposition 2.3.1.** (Itô's lemma for Brownian motions). Consider a twice-differentiable scalar function  $f(t, x)$  of two real variables  $t$  and  $x$ , and let  $\{B_t : t \geq 0\}$  denote a Brownian motion process. Then, for every  $t \geq 0$ ,

$$df(t, B_t) = \frac{\partial f(t, B_t)}{\partial t}dt + \frac{\partial f(t, B_t)}{\partial x}dB_t + \frac{1}{2} \frac{\partial^2 f(t, B_t)}{\partial x^2}dt. \quad (2.23)$$

**Proposition 2.3.2.** (Itô's lemma for Itô processes). Consider a twice-differentiable scalar function  $f(t, x)$  of two real variables  $t$  and  $x$ , and let  $\{X_t : t \geq 0\}$  denote an Itô process. Then, for every  $t \geq 0$ ,

$$\begin{aligned} df(t, X_t) &= \left( \frac{\partial f(t, X_t)}{\partial t} + \mu(t, X_t) \frac{\partial f(t, X_t)}{\partial x} \right) dt + \frac{1}{2} \sigma(t, X_t)^2 \frac{\partial^2 f(t, X_t)}{\partial x^2} dt \\ &\quad + \sigma(t, X_t) \frac{\partial f(t, X_t)}{\partial x} dB_t. \end{aligned} \quad (2.24)$$

### 2.3.5 Discounted Feynman-Kac Theorem

The discounted Feynman-Kac theorem provides a link between stochastic processes and partial differential equations (PDEs). It provides a solution for pricing PDEs and is instrumental in options pricing theory.

**Proposition 2.3.3.** (One-dimensional case). Consider a probability space  $(\Omega, \mathcal{F}, \mathbb{P})$  and suppose that  $\{X_t : t \geq 0\}$  is a stochastic process that satisfies the stochastic differential

equation

$$dX_t = \mu(t, X_t)dt + \sigma(t, X_t)dB_t, \quad (2.25)$$

where  $B_t$  is a standard Brownian motion. Let  $f(t, X_t)$  denote a twice-differentiable function of  $t$  and  $X_t$  that satisfies the following PDE

$$\frac{\partial f(t, x)}{\partial t} + \mu(t, x)\frac{\partial f(t, x)}{\partial x} + \frac{1}{2}\sigma(t, x)^2\frac{\partial^2 f(t, x)}{\partial x^2} - rf(t, x) = 0, \quad (2.26)$$

subject to the terminal condition  $f(T, X_T) = h(X_T)$ . The constant  $r$  denotes a discount factor and  $h(X)$  denotes a Borel-measurable function. Then according to the discounted Feynman-Kac theorem,  $f(t, X_t)$  has the solution

$$f(t, x) = \mathbb{E} \left[ e^{-r(T-t)} h(X_T) \mid X_t = x \right]. \quad (2.27)$$

The discounted Feynman-Kac theorem can be applied in both possible scenarios. In the first case, if the process of  $X_t$  is known and a function  $f(X_t, t)$  is given along with its terminal condition  $f(X_T, T) = h(X_T)$ , then the solution for  $f(X_t, t)$  can be easily obtained. In the second case, if the process  $X_t$  is known, and we know the solution of  $f(X_t, t)$  from the definition, then we can be sure that  $f(X_t, t)$  satisfies the PDE given in the definition.

The multi-dimensional discounted Feynman-Kac theorem is a general extension of the one-dimensional case.

**Proposition 2.3.4.** (Multi-dimensional case). Consider a probability space  $(\Omega, \mathcal{F}, \mathbb{P})$  and suppose  $\{\mathbf{X}_t : t \geq 0\}$  denotes an  $n$ -dimensional stochastic process that satisfies the

$n$ -dimensional stochastic differential equation

$$d\mathbf{X}_t = \boldsymbol{\mu}(t, \mathbf{X}_t)dt + \boldsymbol{\sigma}(t, \mathbf{X}_t)d\mathbf{B}_t, \quad (2.28)$$

where  $\mathbf{B}_t$  is an  $m$ -dimensional standard Brownian motion,  $\boldsymbol{\mu}(t, \mathbf{X}_t)$  is an  $n$ -dimensional vector and  $\boldsymbol{\sigma}(t, \mathbf{X}_t)$  is an  $n \times m$  matrix. Let  $f(t, \mathbf{X}_t)$  denote a twice-differentiable function of  $t$  and  $\mathbf{X}_t$  that satisfies the following PDE

$$\frac{\partial f(t, \mathbf{x})}{\partial t} + \sum_{i=1}^n \mu_i(t, x) \frac{\partial f(t, \mathbf{x})}{\partial x_i} + \frac{1}{2} \sum_{i=1}^n \sum_{j=1}^n [\boldsymbol{\sigma}(t, \mathbf{x})\boldsymbol{\sigma}(t, \mathbf{x})^T]_{ij} \frac{\partial^2 f(t, \mathbf{x})}{\partial x_i \partial x_j} - rf(t, \mathbf{x}) = 0, \quad (2.29)$$

subject to the terminal condition  $f(T, \mathbf{X}_T) = h(\mathbf{X}_T)$ . Then according to the discounted Feynman-Kac theorem,  $f(t, \mathbf{X}_t)$  has the solution

$$f(t, \mathbf{x}) = \mathbb{E} \left[ e^{-r(T-t)} h(\mathbf{X}_T) \mid \mathbf{X}_t = \mathbf{x} \right]. \quad (2.30)$$

## Chapter 3

# Price Dynamics of LETFs

This chapter presents the discrete and continuous time models that relate the price of an LETF to the value of its underlying index. The continuous-time model undergoes empirical analysis and is tested for consistency among various equity and volatility LETFs with different leverage ratios. LETFs of the S&P 500, NASDAQ 100 and DJIA equity indices are used for testing, along with a few LETFs of the VIX. The pricing model that links an LETF to its underlying index exhibits a volatility decay factor which is studied in depth. Another study involves long-term empirical leverage ratio estimation by applying an optimization technique, which uses historical data to minimize the leverage ratio of various LETFs. The results are compared with leverage ratio values obtained through linear regression.

### 3.1 Modelling Returns of Leveraged ETFs

The theoretical return of an LETF is illustrated as

$$L_n = L_0 \prod_{j=1}^n (1 + \beta R_j), \quad (3.1)$$

where  $L_n$  is the price of an LETF on day  $n$ ,  $\beta$  is the leverage ratio and  $R_j$  is the daily return of the reference index. Equation (3.1) is known as the leverage benchmark and is used in empirical analysis to test the consistency of existing LETFs, to compare pricing models and to test portfolios replicating LETFs.

The popularity of LETFs stems from their ability to amplify short-term returns for investors. Intuitively, if an asset or index is bullish, investors would like to hold a bullish LETF with a strong ratio. Similarly, a bearish index will provide highest returns with a highly negative bearish LETF. Mathematically, this can be explained by taking the derivative of the log of Equation (3.1) with respect to  $\beta$

$$\frac{d}{d\beta} \left[ \ln \left( \frac{L_n}{L_0} \right) \right] = \sum_{j=1}^n \frac{R_j}{1 + \beta R_j}. \quad (3.2)$$

Equation (3.2) mathematically illustrates the instinctive use of LETFs under different market conditions. For a bullish LETF  $\beta > 0$ , if  $R_j > 0$  for all  $j$ , then  $\log(\frac{L_n}{L_0})$ , and therefore the value of  $L_n$ , is increasing in  $\beta$ . In other terms, a larger positive leverage ratio is necessary for higher returns when the reference asset is increasing in value. On the other hand, if  $R_j < 0$  for all  $j$ , and  $\beta < 0$ , a more negative  $\beta$  increases  $\log(\frac{L_n}{L_0})$  and thus  $L_n$ . Therefore, when the reference asset is decreasing in value, a larger negative bullish LETF is preferred to yield higher returns.

Day	ETF	Return (%)	2x LETF	Return (%)	-2x LETF	Return (%)
0	100	-	100	-	100	-
1	95	-5%	90	-10%	110	10%
2	99.75	5%	99	10%	99	-10%
3	94.76	-5%	89.10	-10%	108.90	10%
4	99.50	5%	98.01	10%	98.01	-10%
5	94.53	-5%	88.21	-10%	107.81	10%
6	99.26	5%	97.03	10%	97.03	-10%

Table 3.1: Daily rebalancing of LETFs.

Despite both long and short LETFs being designed to move in opposite directions

to one another, it is possible for both LETFs to have a negative cumulative return over a long holding period. Table 3.1 illustrates this for a 6-day holding period where the return column indicates the percentage return on a given day. Notice that after 6 days, all three portfolios are at a loss, despite the -2x LETF portfolio having the opposite return on any given day. You would think that if the bullish LETF is at a loss after 6 days, the bearish LETF would be in profit, but this is not the case. This is the effect of daily rebalancing. In fact, the underlying ETF loses 0.74% of its value after 6 days, but both its bullish and bearish LETFs are at a loss of 2.97%, more than four times larger.

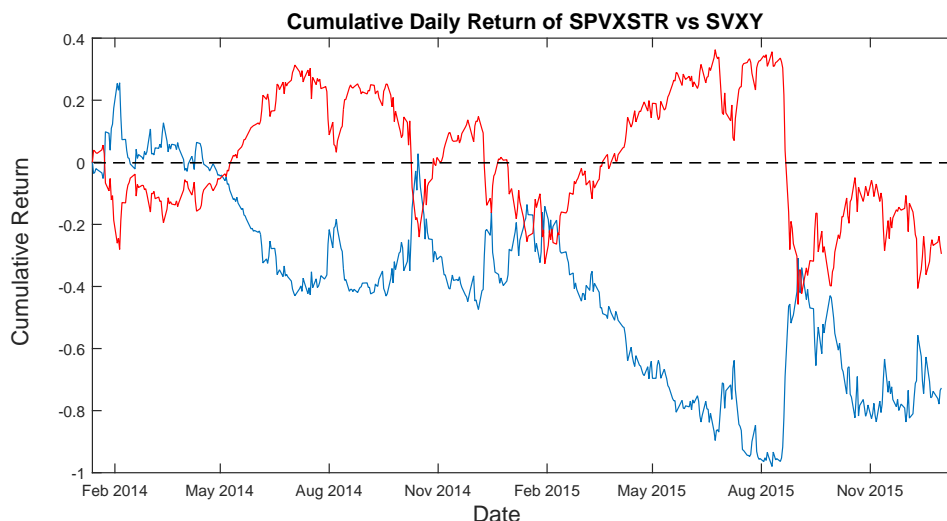


Figure 3.1: Cumulative log-return of SPVXSTR (blue) and SVXY (red).

Figure 3.1 illustrates this point visually by comparing the cumulative returns of the VIX short-term futures index return, SPVXSTR, and an inverse (-1x) LETF of this index, SVXY, over a two-year holding period. The figure shows multiple occasions when both the inverse LETF and its reference index are significantly in losses. There is a constant decay in the performance of SVXY and it is larger when the reference index is losing value and also during periods of high volatility. This phenomenon is a result of daily portfolio rebalancing and is a strong argument against holding LETFs for long periods.

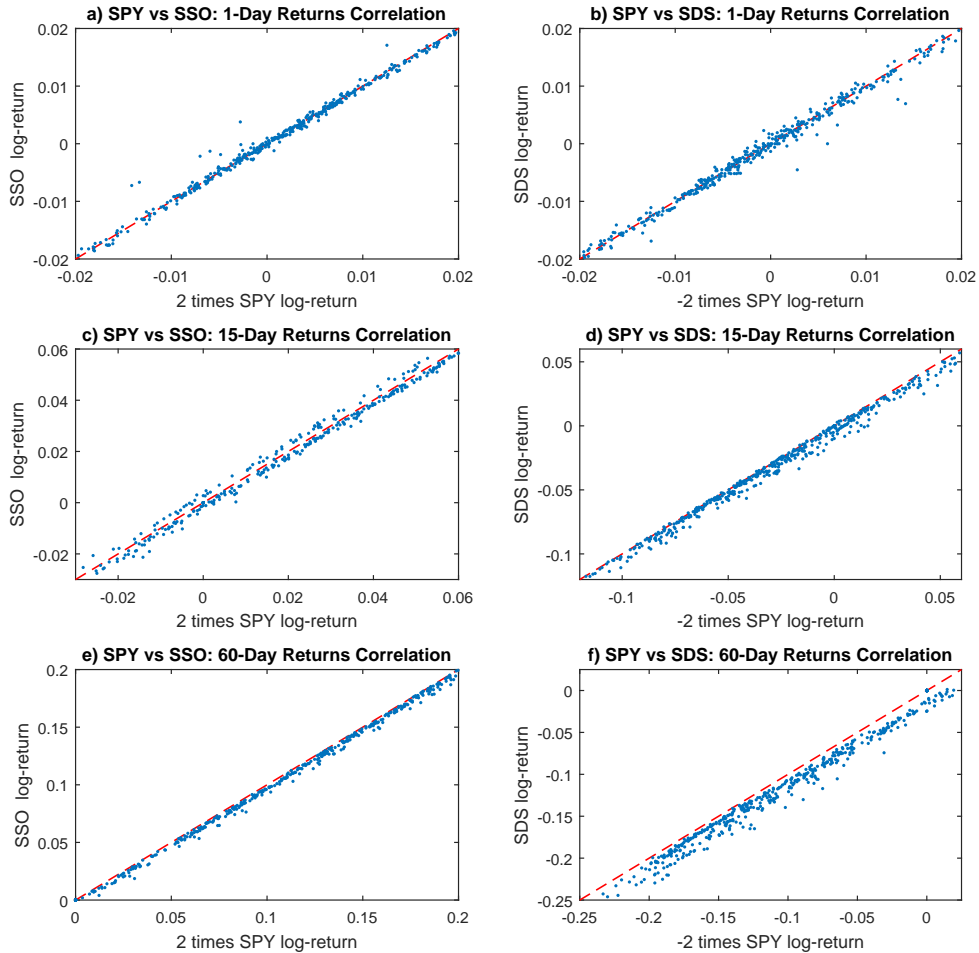


Figure 3.2: Empirical and theoretical returns comparison for various holding periods of  $\pm 2x$  LETFs.

As mentioned earlier, the value erosion becomes larger as the holding period increases and also impacts higher absolute leverage ratios more, due to higher deviance from the reference asset being amplified over a long time horizon. Figures 3.2 and 3.3 illustrate this by looking at the empirical returns of four S&P 500 LETFs over different holding periods. The LETFs have leverage ratios of 2, -2, 3 and -3. These figures illustrate the correlation between these LETFs and SPY, the largest traded ETF of S&P 500. The SPY returns are scaled with respect to the leverage ratio of the ETF it is

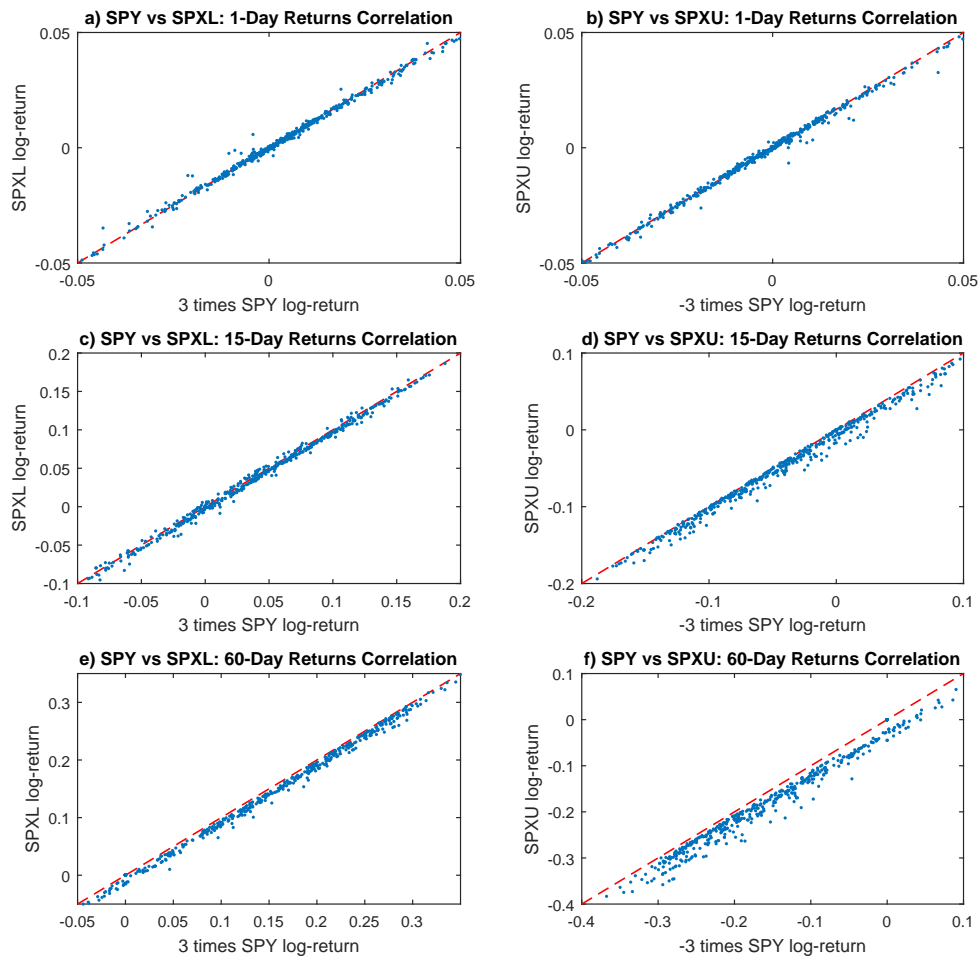


Figure 3.3: Empirical and theoretical returns comparison for various holding periods of  $\pm 3x$  LETFs.

paired with. Theoretically, without any expense fees and volatility decay, the returns should spread evenly along the dotted red line. The figures shows an increase in spread with a longer holding period as expected, but the returns are also below the theoretical value in almost all 15-day and 60-day holding periods, illustrating the volatility decay for longer holding periods. The figures also show significantly higher volatility decay for inverse LETFs, and also for larger absolute leverage ratio values.

### 3.1.1 Continuous-Time Model

Denoting the reference index as  $\{S_t : t \geq 0\}$ , its price evolution is modeled by the stochastic differential equation

$$dS_t = S_t(\mu_t dt + \sigma_t dB_t), \quad (3.3)$$

where  $\{B_t : t \geq 0\}$  is a standard Brownian motion term under the physical measure  $\mathbb{P}$ . The stochastic drift  $\{\mu_t : t \geq 0\}$  represents the time-varying mean rate of return, and  $\{\sigma_t : t \geq 0\}$  is the instantaneous stochastic price volatility. To simply illustrate the relationship between LETFs and its underlying index, this chapter does not specify a parametric stochastic volatility model, although Chapter 4 introduces an extension of the Heston stochastic volatility model which accounts for the path-dependent property of an LETF, for the purpose of options pricing.

Using the reference index  $S_t$ , a long LETF  $L_t$  with  $\beta \geq 1$  is constructed through a portfolio where  $\beta L_t$  is invested in the reference index  $S_t$  and  $(\beta - 1)L_t$  is borrowed at the interest rate  $r$ . An expense fee,  $f$ , is charged for the purchase of shares. Similarly, a short LETF with  $\beta \leq -1$  is constructed by entering a short position of  $|\beta L_t|$  in  $S_t$  and holding  $(1 - \beta)L_t$  at the risk-free rate. Short LETFs in general also incur a fee proportional to the rate of borrowing, when short selling. This extra charge is omitted in our model.

With knowledge of this constant proportion trading strategy, we can mathematically illustrate the price dynamics of a  $\beta$ -LETF in terms of its underlying index as

$$dL_t = L_t \beta \frac{dS_t}{S_t} + L_t((1 - \beta)r - f)dt. \quad (3.4)$$

**Proposition 3.1.1.** (Relationship between ETF and underlying index). Based on the price dynamics of an ETF from Equation (3.4), the price of an ETF  $L_t$  is linked to its reference index  $S_t$  as follows

$$\ln\left(\frac{L_t}{L_0}\right) = \beta \ln\left(\frac{S_t}{S_0}\right) + \frac{\beta - \beta^2}{2} \int_0^t \sigma_u^2 du + ((1 - \beta)r - f)t \quad (3.5)$$

*Proof.* Equation (3.5) is derived by applying Itô's lemma to (3.3) and (3.4).

$$\begin{aligned} d \ln L_t &= \frac{dL_t}{L_t} - \frac{1}{2} \left\langle \frac{dL_t}{L_t}, \frac{dL_t}{L_t} \right\rangle \\ &= \beta \frac{dS_t}{S_t} + ((1 - \beta)r - f)dt - \frac{\beta^2}{2} \left\langle \frac{dS_t}{S_t}, \frac{dS_t}{S_t} \right\rangle \\ &= \beta \frac{dS_t}{S_t} + ((1 - \beta)r - f)dt - \frac{\beta^2}{2} \sigma_t^2 dt. \end{aligned}$$

Similarly, we get

$$d \ln S_t = \frac{dS_t}{S_t} - \frac{1}{2} \sigma_t^2 dt \Rightarrow \frac{dS_t}{S_t} = d \ln S_t + \frac{1}{2} \sigma_t^2 dt.$$

Substituting for  $\frac{dS_t}{S_t}$  into  $d \ln L_t$  gives

$$\begin{aligned} d \ln L_t &= \beta d \ln S_t + \frac{\beta}{2} \sigma_t^2 dt + ((1 - \beta)r - f)dt - \frac{\beta^2}{2} \sigma_t^2 dt \\ &= \beta d \ln S_t + \frac{\beta - \beta^2}{2} \sigma_t^2 dt + ((1 - \beta)r - f)dt. \end{aligned}$$

Finally, integrating both sides with respect to  $t$  from 0 to  $t$  gives the desired result

$$\ln\left(\frac{L_t}{L_0}\right) = \beta \ln\left(\frac{S_t}{S_0}\right) + \frac{\beta - \beta^2}{2} \int_0^t \sigma_u^2 du + ((1 - \beta)r - f)t.$$

□

It is important to note the second term in (3.5)

$$\frac{\beta - \beta^2}{2} < 0 \quad \text{for } \beta \neq 0 \text{ or } \beta \neq 1,$$

which illustrates that the value erosion in LETF log-returns is proportional to the realized variance of the underlying index  $\int_0^t \sigma_u^2 du$ . This erosion, or volatility decay, affects both positive and negative leverage ratios and is significantly stronger for short LETFs of the same magnitude as their long counterparts. With variance increasing over time, this volatility decay also increases in absolute value over longer time periods, as previously illustrated.

### 3.1.2 Empirical Validation

This section attempts to justify the relationship between an LETF and its underlying index as modeled in Equation (3.5). The empirical study includes 15 different LETFs of the S&P 500, NASDAQ 100 and DJIA indices as well as 2 VIX LETFs. The data sample for each index was procured from Thomson Reuters Datastream package, and contains the closing prices from 2<sup>nd</sup> January 2013 to 29<sup>th</sup> December 2017.

Table 3.2 lists the LETFs used for empirical analysis along with their  $\beta$  values and expense ratio. While the option pricing model in Chapter 4 disregards this expense ratio, this chapter compares the model in Equation (3.5) with the expense ratio to get a fair analysis of the model.

The VIX LETFs chosen for this study are designed to track the VIX Short-Term Futures Total Return Index (SPVXSTR). The inverse LETF, SVXY, has gained major criticism since February 2018, when the value of its shares, and the value of similar inverse LETFs, dropped by up to 90% during after-hours trading on February 5<sup>th</sup>, 2018. This depreciation of value was caused by a large, unprecedented spike in the VIX. Due to the controversy, the LETF was altered to provide -0.5x the return, reducing its

Reference Index	LETF Ticker	Leverage Ratio	Expense Ratio (%)
S&P 500 (^GSPC)	SSO	+2	0.90
	SPXL	+3	1.04
	SH	-1	0.89
	SDS	-2	0.89
	SPXU	-3	0.90
NASDAQ (^NDX)	QLD	+2	0.95
	TQQQ	+3	0.95
	PSQ	-1	0.95
	QID	-2	0.95
	SQQQ	-3	0.95
Dow Jones Industrial Average (^DJI)	DDM	+2	0.95
	UDOW	+3	0.95
	DOG	-1	0.95
	DXD	-2	0.95
	SDOW	-3	0.95
VIX Short-Term Futures Total Return (^SPVXSTR)	UVXY	+2	1.65
	SVXY	-1	1.38

Table 3.2: Data description.

risk during market instability, but also its potential reward. The data accumulated for analysis is prior to this incident, and therefore we consider SVXY to provide 1x the return, as it did.

On 12 January 2017, UDOW reverse-split its shares 1-for-4, increasing its price from approximately \$10 to \$40. Since this split would falsely impact the returns of any holding periods containing this split, it would provide inconsistent empirical results. Therefore, the data prior to this split was altered by amplifying its daily closing prices prior to the split by four times. Since our analysis uses the log-return of closing prices and not the daily closing values, this alteration would only affect one data point.

The empirical verification of Equation (3.5) is done by approximating the tracking error between the empirical LETF log-returns using our data sample, and the theoretical

log-returns from the model

$$\epsilon_t = \ln \frac{L_t}{L_0} - \beta \ln \frac{S_t}{S_0} + \frac{\beta - \beta^2}{2} V_t + ((1 - \beta)r - f)t, \quad (3.6)$$

where  $t = \frac{1}{252}$  represents one day, and the realized variance,  $V_t$ , at time  $t$  is computed as the accumulated variance from each day up to the current time. The theoretical LETF prices are simulated using reference index prices from 2<sup>nd</sup> January 2013 to 29<sup>th</sup> December 2017. The respective expense ratios from Table 3.2 are applied to each LETF. The interest rate is set at 1.7% as per the 3-month LIBOR rate published by the Federal Reserve Bank. In the case of short LETFs, the rate of borrowing is ignored.

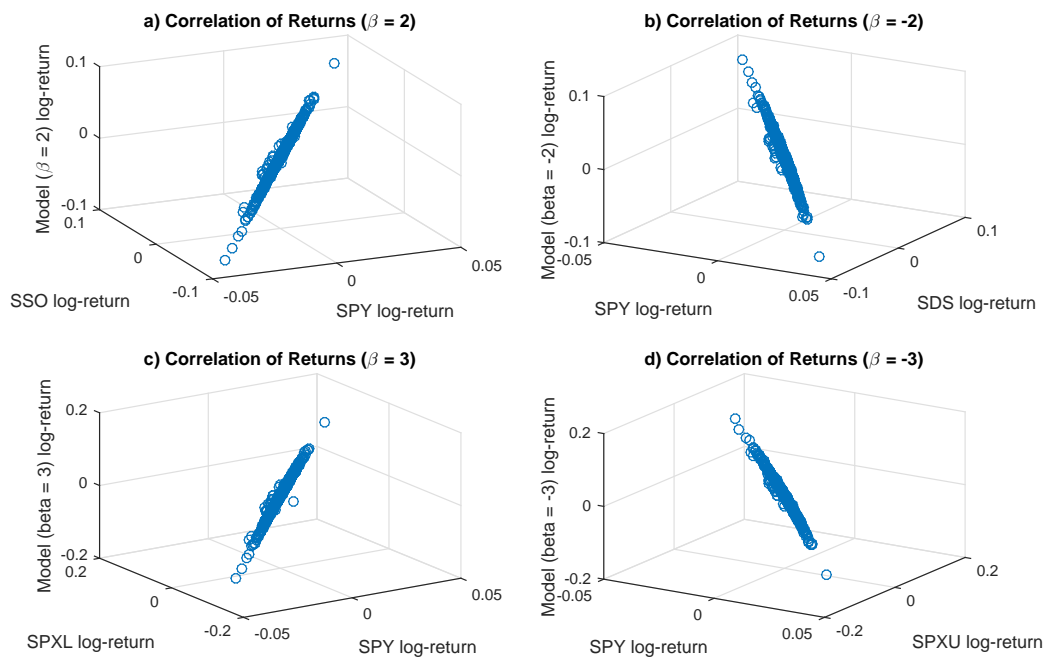


Figure 3.4: Correlation in log-returns of SPY and the  $\pm 2x$  and  $\pm 3x$  LETFs with their respective theoretical values.

Figure 3.4 illustrates the three-way correlation between SPY, an ETF of S&P 500, and different leveraged ETFs of the S&P 500 with their theoretical values determined using Equation (3.5). As expected, the LETFs and their theoretical counterparts show

strong positive correlation, in the case of bullish LETFs, and strong negative correlation, for bearish LETFs, with their underlying ETF. Furthermore, there is a consistently strong positive relationship between the theoretical and empirical log-returns of the LETF in each sub-figure. The minor deviancies are calculated using Equation (3.6) and shown in Table 3.3 below.

Reference Index	LETF Ticker	Average Tracking Error (%)	Standard Deviation (%)
^GSPC	SSO	1.43	6.84
	SPXL	0.83	24.96
	SH	-1.45	4.33
	SDS	-2.37	7.76
	SPXU	-3.37	12.52
^NDX	QLD	0.68	6.74
	TQQQ	0.77	10.83
	PSQ	-1.30	4.49
	QID	-2.41	8.63
	SQQQ	-3.87	11.88
^DJI	DDM	1.62	11.05
	UDOW	2.85	17.91
	DOG	-1.52	7.85
	DXD	-2.76	11.91
	SDOW	-3.94	12.58
^SPVXSTR	UVXY	-9.15	205.19
	SVXY	-10.17	113.52

Table 3.3: Tracking error (%) of theoretical and empirical LETF returns.

Table 3.3 lists the average tracking error of each LETF along with its standard deviation. As the table shows, the tracking error in most cases is minute and illustrates the accuracy of the LETF pricing model. The VIX LETFs in the last two rows show higher errors than the equity LETFs and this can be attributed to the higher unpredictability of their underlying index as well as their tendency to fluctuate during periods of high volatility. Both VIX LETFs have an average tracking error of approximately 10%, with extremely large deviations from the mean, as their standard deviation values are 205.19% and 113.52%, for UVXY and SVXY, respectively. On the other hand, the

model responds fairly well to equity LETFs. The average tracking error for bullish LETFs is generally lower than those for bearish LETFs. Across the table, the NASDAQ bullish LETFs fit the model the best as QLD and TQQQ provide the closest results to their theoretical values with tracking errors of 0.68% and 0.77%, respectively. We can conclude from these results that Equation (3.5) provides a reasonable estimate of an LETF price based on the price of its underlying index, regardless of the leverage ratio.

### 3.2 Empirical Leverage Ratio Analysis

In the previous section, the leverage ratio  $\beta$  has been assumed to be accurate as advertised. Though ETF providers attempt to target a given leverage ratio, there can be certain discrepancies between the advertised and empirical ratios. This section uses a method introduced by Leung and Santoli [15] to track empirical ratios and provides a replication technique to achieve a precise ratio.

In discrete time, with  $\Delta t = \frac{1}{252}$ , the  $n$ -day log-return of the LETF is given by

$$\ln \frac{L_{t+n\Delta t}}{L_t} = \beta \ln \frac{S_{t+n\Delta t}}{S_t} + \theta V_t^{(n)} + ((1 - \beta)r - f)n\Delta t, \quad (3.7)$$

where the realized variance is computed as

$$V_t^{(n)} = \sum_{i=0}^{n-1} (R_{t+i\Delta t}^S - \hat{R}_t^S)^2, \quad \text{with} \quad \hat{R}_t^S = \frac{1}{N} \sum_{i=0}^{N-1} R_{t+i\Delta t}^S, \quad (3.8)$$

where  $R_t^S$  is the daily return of the reference index at time  $t$ . The theoretical value of  $\theta$  is

$$\theta = \frac{\beta - \beta^2}{2}.$$

The discretized LETF log-return from Equation (3.7) has a linear regression of the

form

$$\ln \frac{L_t}{L_0} = \hat{\beta} \ln \frac{S_t}{S_0} + \hat{\theta} V_t + \hat{c} + \epsilon, \quad (3.9)$$

where  $V_t = \int_0^t \sigma_u^2 du$  and  $\epsilon \sim N(0, 1)$ .

Historical LETF prices and reference index prices can be applied to this regression to estimate the constant coefficients  $\hat{\beta}$ ,  $\hat{\theta}$  and  $\hat{c}$ . However, the coefficient estimates provided through this approach may not be reliable due to the strong dependence between  $V_t$  and  $\ln S_t$ . This issue of collinearity was studied and illustrated using various LETFs by Guo and Leung [12].

There is another problem that arises with the use of this model. Estimates for the coefficients  $\hat{\beta}$  and  $\hat{\theta}$  can be found through regression, but  $\theta$  also has a theoretical value in terms of  $\beta$  i.e.,  $\theta = \beta(1 - \beta)/2$ , with no guarantee that  $\hat{\theta}$  from the regression would be equal to the theoretical value using  $\hat{\beta}$ . This essentially leads to two sets of results for  $\hat{\theta}$  and  $\hat{\beta}$  with no appropriate way to confirm the correct estimates aside from empirical accuracy. Guo and Leung [12] illustrated this dilemma, and their results showed significant deviation in the two sets of estimates, which led to doubt about the reliability of this method.

The drawbacks of the linear regression method led Leung and Santoli [15] to search for an alternate technique to estimate the empirical leverage ratio with the objective of finding a single optimized estimate. With this in mind, an optimization technique was used to minimize the sum of squared differences between the realized and theoretical LETF log-returns using the discrete model in Equation (3.7). The optimization problem is formulated as

$$\min_{\beta \in \mathbb{R}} \sum_{i=1}^n (y_i - f_i(\beta))^2, \quad (3.10)$$

where  $y_1, \dots, y_n$  are the empirical log-returns of the LETF, and  $f_i(\beta), \dots, f_n(\beta)$  are the theoretical returns given by

$$\begin{aligned} f_i(\beta) &= \beta x_i - \frac{\beta(\beta-1)}{2} v_i + ((1-\beta)r - f)\Delta t \\ &= \beta(x_i - (r-f)\Delta t) - \frac{\beta(\beta-1)}{2} v_i + (r-f)\Delta t, \end{aligned} \quad (3.11)$$

where each  $f_i(\beta)$  requires the log-return of the reference  $x_i$ , and the realized variance  $v_i$  over the same period of length  $\Delta t$ . The optimal leverage ratio can be found by applying the first-order optimality condition

$$\sum_{i=1}^n (y_i - f_i(\beta))(x_i - (r-f)\Delta t - \beta v_i + \frac{1}{2}v_i) = 0. \quad (3.12)$$

Expanding the left-hand side gives

$$\begin{aligned} & \sum_{i=1}^n (y_i - f_i(\beta))(x_i - (r-f)\Delta t - \beta v_i + \frac{1}{2}v_i) \\ &= \sum_{i=1}^n (y_i - \beta(x_i - (r-f)\Delta t) + \frac{\beta^2}{2}v_i - \frac{\beta}{2}v_i - (r-f)\Delta t)(x_i - (r-f)\Delta t - \beta v_i + \frac{1}{2}v_i) \\ &= \sum_{i=1}^n (y_i - (r-f)\Delta t - \beta(x_i - (r-f)\Delta t + \frac{v_i}{2}) + \frac{\beta^2}{2}v_i)(x_i - (r-f)\Delta t - \beta v_i + \frac{1}{2}v_i) \\ &= \left( -\sum_{i=1}^n \frac{v_i^2}{2} \right) \beta^3 + \left( \sum_{i=1}^n \frac{3}{2}(x_i - (r-f)\Delta t)v_i + v_i^2 \right) \beta^2 \\ &+ \left( \sum_{i=1}^n -((x_i - (r-f)\Delta t) + \frac{1}{2}v_i)^2 + v_i((r-f)\Delta t - y_i) \right) \beta \\ &+ \left( \sum_{i=1}^n (y_i - (r-f)\Delta t)((x_i - (r-f)\Delta t) + \frac{1}{2}v_i) \right). \end{aligned}$$

The optimality condition then reduces to the cubic equation

$$A\beta^3 + B\beta^2 + C\beta + D = 0, \quad (3.13)$$

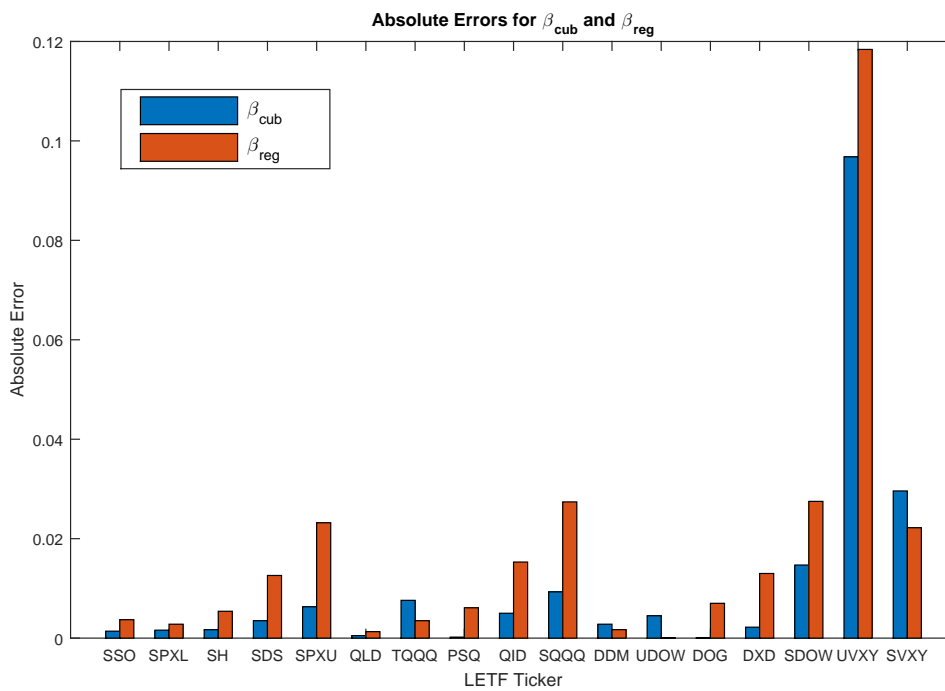
where the constant coefficients are given by

$$\begin{aligned}
 A &= -\sum_{i=1}^n \frac{v_i^2}{2}, \\
 B &= \sum_{i=1}^n \frac{3}{2} (x_i - (r - f)\Delta T)v_i + v_i^2, \\
 C &= \sum_{i=1}^n -\left((x_i - (r - f)\Delta T) + \frac{1}{2}v_i\right)^2 + v_i((r - f)\Delta T - y_i), \\
 D &= \sum_{i=1}^n (y_i - (r - f)\Delta T)\left((x_i - (r - f)\Delta T) + \frac{1}{2}v_i\right).
 \end{aligned}$$

The cubic polynomial from Equation (3.13) is solved numerically using MATLAB for our LETFs from Table 3.2. Table 3.4 displays the empirical  $\beta$  estimates from both methods along with the absolute error of these values calculated for 5-day holding periods. For the most part, both methods provide reasonably close estimates to the advertised  $\beta$  values, with the exception of the VIX LETFs in the last three rows, which produced significantly larger errors, possibly due to their unpredictable behavior compared to equity LETFs. The optimization estimates,  $\beta_{cub}$ , generally produced lower errors compared to  $\beta_{reg}$ , justifying its reliability over regression, considering the other drawbacks of regression as discussed previously. The table shows no real pattern in errors with respect to  $\beta$  values, but in most cases, negative LETFs have higher errors than their positive counterparts, especially with the regression method. Figure 3.5 illustrates the absolute errors from both methods as a bar chart for better visual representation.

Equation (3.5) shows the dependence of LETF returns on not only the underlying asset returns but also the accumulated variance of the underlying asset. Therefore, to estimate the leverage ratio, we must partition our full sample into  $n$ -day subintervals and compute the realized variance for each subinterval. This method leads to serious disadvantages while using the linear regression, since a short sample period, for example, one or two years, would yield an insufficient amount of data points for regression. This

LETF Ticker	$\beta$	Empirical $\beta$		Absolute Error	
		$\beta_{cub}$	$\beta_{reg}$	$\beta_{cub}$	$\beta_{reg}$
SSO	+2	2.0014	1.9963	0.0014	0.0037
SPXL	+3	3.0016	2.9972	0.0016	0.0028
SH	-1	-1.0017	-0.9946	0.0017	0.0054
SDS	-2	-1.9965	-1.9874	0.0035	0.0126
SPXU	-3	-2.9927	-2.9768	0.0063	0.0232
QLD	+2	2.0005	1.9987	0.0005	0.0013
TQQQ	+3	3.0076	3.0035	0.0076	0.0035
PSQ	-1	-1.0002	-0.9939	0.0002	0.0061
QID	-2	-1.9950	-1.9847	0.0050	0.0153
SQQQ	-3	-2.9907	-2.9726	0.0093	0.0274
DDM	+2	2.0028	2.0017	0.0028	0.0017
UDOW	+3	3.0045	3.0001	0.0045	0.0001
DOG	-1	-0.9999	-0.9930	0.0001	0.0070
DXD	-2	-1.9978	-1.9870	0.0022	0.0130
SDOW	-3	-2.9853	-2.9725	0.0147	0.0275
UVXY	+2	1.9032	1.8816	0.0968	0.1184
SVXY	-1	-0.9704	-0.9778	0.0296	0.0222

Table 3.4: Empirical  $\beta$  estimates from optimization ( $\beta_{cub}$ ) and regression ( $\beta_{reg}$ ) methods.Figure 3.5: Visual representation of estimation errors of  $\beta_{cub}$  and  $\beta_{reg}$ .

issue is mostly relevant to LETFs that were introduced recently. If we create subintervals of longer periods, for example, yearly quarters, this can also impact LETFs with longer history.

A major strength of the optimization technique in this section, compared to the linear regression method, is that a large sample period is not necessary to provide accurate empirical results. This is mainly due to the fact that the optimization technique finds a single variable  $\beta_{cub}$  by minimizing a univariate quadratic function. And the other variable,  $\theta_{cub}$ , can be instantly found using the relationship  $\theta_{cub} = (\beta_{cub} - \beta_{cub}^2)/2$ , which guarantees a consistent result. As discussed previously, the linear regression technique provides two different sets of results and then requires us to find the optimal set, which is not a consistent technique. For example, for one LETF, the optimal set may be created by solving  $\beta_{reg}$  through regression and using the relationship between  $\beta_{reg}$  and  $\theta$  to solve for the latter, whereas another LETF's optimal set could be found by solving for both variables,  $\beta_{reg}$  and  $\theta_{reg}$ , through regression.

Another important empirical test relating to leverage ratios would be to examine how they react to different market conditions. In other words, investors would like to know how the returns of their LETF portfolios will vary when the underlying asset is bullish or bearish. To test this, we can separate our sample into  $n$ -day intervals as before and further divide the sample into two groups, according to whether the  $n$ -day returns are positive or negative. We can then apply the same cubic root-finding method for each group individually and get an accurate estimate for  $\beta$  values conditioned on the sign of the returns.

Table 3.5 shows the variation in estimated  $\beta$  values depending on market conditions.  $\beta_{cub}^+$  estimates  $\beta$  values when the underlying index has positive returns over a 5-day holding period. Similarly,  $\beta_{cub}^-$  estimates  $\beta$  when the underlying index has negative returns. The absolute error in this case measures the absolute difference between the new estimates dependent on market conditions and the previous estimate  $\beta_{cub}$ . In general,

LETF Ticker	$\beta$	$\beta_{cub}$	$\beta_{cub}^+$	Absolute Error	$\beta_{cub}^-$	Absolute Error
SSO	+2	2.0014	2.0792	0.0078	1.9221	0.0793
SPXL	+3	3.0016	3.1783	0.1767	2.8312	0.1704
SH	-1	-1.0017	-1.0176	0.0159	-0.9752	0.0265
SDS	-2	-1.9965	-1.9743	0.0222	-1.9940	0.0025
SPXU	-3	-2.9927	-2.8960	0.0967	-3.0480	0.0553
QLD	+2	2.0005	2.0456	0.0451	1.9472	0.0533
TQQQ	+3	3.0076	3.1151	0.1075	2.8872	0.1204
PSQ	-1	-1.0002	-1.0145	0.0143	-0.9738	0.0264
QID	-2	-1.9950	-1.9846	0.0104	-1.9765	0.0185
SQQQ	-3	-2.9907	-2.9321	0.0587	-2.9952	0.0045
DDM	+2	2.0028	2.0848	0.0820	1.9165	0.0863
UDOW	+3	3.0045	3.2019	0.1974	2.8129	0.1925
DOG	-1	-0.9999	-1.0192	0.0193	-0.9664	0.0335
DXD	-2	-1.9978	-1.9756	0.0222	-1.9906	0.0072
SDOW	-3	-2.9853	-2.8940	0.0913	-3.0278	0.0425
UVXY	+2	1.9032	1.9112	0.0080	1.9467	0.0435
SVXY	-1	-0.9704	-0.9104	0.0600	-0.9828	0.0124

Table 3.5: Comparison of empirical  $\beta$  estimates during positive and negative return periods.

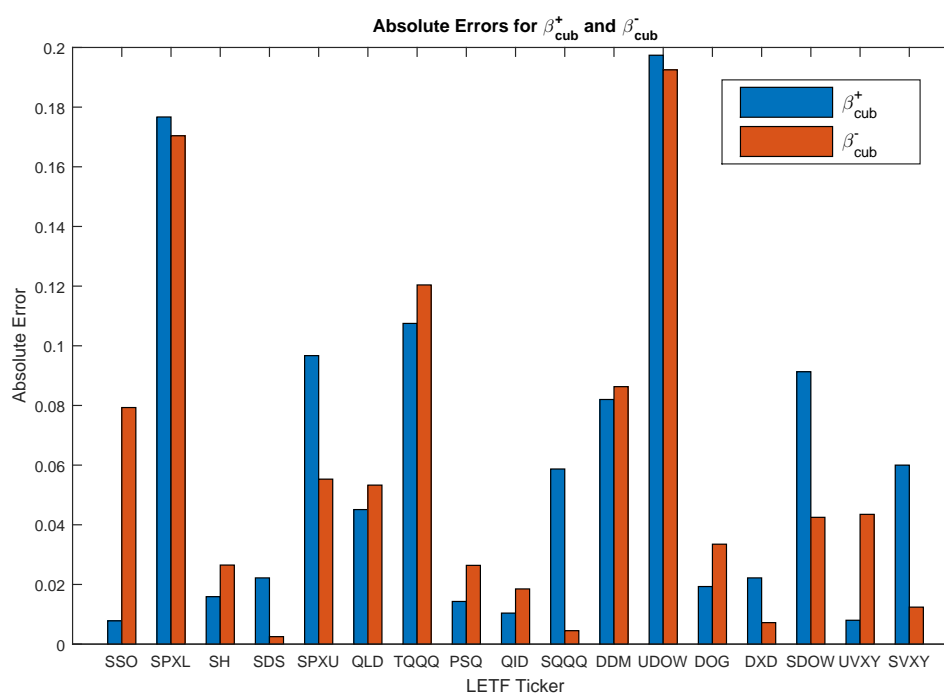


Figure 3.6: Visual representation of estimation errors of  $\beta_{cub}^+$  and  $\beta_{cub}^-$ .

$\beta_{cub}^+$  exceeds  $\beta_{cub}$  for bullish LETFs and underperforms with bearish LETFs. On the other hand,  $\beta_{cub}^-$  seems to mostly underperform relative to  $\beta_{cub}$ . While the absolute error seems to be low in most cases, for positive LETFs the error seems to increase for higher leveraged ETFs, for both  $\beta_{cub}^+$  and  $\beta_{cub}^-$ . For negative LETFs, there is no conclusive pattern in errors. Figure 3.6 provides a bar chart for better visual representation of these errors.

## Chapter 4

# LETFS Option Pricing

This chapter provides an analytical solution for the price of a European call option of an LETF. The value of an LETF's underlying index,  $S_t$ , is assumed to follow Heston dynamics and an additional process is created to account for the LETF's path-dependent property. After deriving the pricing PDE of the underlying index, the characteristic function of an LETF is obtained. Using this, we apply the Carr-Madan Fourier transform method to obtain our call price function.

### 4.1 Heston Stochastic Volatility Model

This section introduces the Heston stochastic volatility model and provides the joint MGF of the underlying index, its volatility and the path dependent process. The joint MGF, which is given an exponential affine form, is derived analytically in Section 4.2. The joint MGF is essentially a link to the characteristic function of an LETF, which is necessary to formulate a call price model for LETFs.

Under a risk-neutral probability measure  $\mathbb{Q}$ , assume that  $S_t$  follows the Heston

dynamics

$$\begin{aligned} dS_t &= (r - q)S_t dt + \sqrt{v_t}S_t dB_t^{(1)}, \\ dv_t &= \kappa(\theta - v_t)dt + \sigma\sqrt{v_t}dB_t^{(2)}, \end{aligned} \quad (4.1)$$

where,  $\text{corr}(dB_t^{(1)}, dB_t^{(2)}) = \rho dt$ ,  $r$  is the risk-free rate,  $q$  is the dividend yield,  $\kappa$  is the mean-reverting speed,  $\theta$  is the long-term mean of variance,  $\sigma$  is the volatility of volatility and  $v_t$ , the variance of the underlying index, is a Cox-Ingersoll-Ross (CIR) process [9].

The path-dependant property of an LETF implies another variable to describe the evolution of the volatility  $v_t$

$$dy_t = v_t dt, \quad (4.2)$$

where  $y_t = \int_0^t v_u du$  and  $y_0 = 0$ .

Suppose  $x_t = \ln S_t$ . Using Itô's lemma we can obtain its process

$$\begin{aligned} dx_t &= d \ln S_t = \frac{\partial \ln S_t}{\partial t} dS_t + \frac{1}{2} \frac{\partial^2 \ln S_t}{\partial t^2} \langle dS_t, dS_t \rangle \\ &= \frac{1}{S_t} \left[ (r - q)S_t dt + \sqrt{v_t}S_t dB_t^{(1)} \right] - \frac{1}{2S_t^2} \left[ v_t S_t^2 dt \right] \\ &= \left( r - q - \frac{1}{2}v_t \right) dt + \sqrt{v_t} dB_t^{(1)}. \end{aligned} \quad (4.3)$$

Combining (4.1), (4.2) and (4.3), we get the following system which defines the log-price and variance dynamics of the underlying index

$$\begin{cases} dx_t = (r - q - \frac{1}{2}v_t)dt + \sqrt{v_t}dB_t^{(1)}, \\ dv_t = \kappa(\theta - v_t)dt + \sigma\sqrt{v_t}dB_t^{(2)}, \\ dy_t = v_t dt. \end{cases} \quad (4.4)$$

Suppose  $[x_t, v_t, y_t]^T$  is a vector, where  $t$  is the present time and all information up to time  $t$  is known for these processes, then its joint MGF is

$$f(t, x, v, y; z_1, z_2, z_3) = \mathbb{E}^{\mathbb{Q}}[e^{z_1 x_T + z_2 v_T + z_3 y_T} | x_t = x, v_t = v, y_t = y], \quad (4.5)$$

where  $z_1, z_2$  and  $z_3$  are constants. Note that the joint MGF at time  $T$  is

$$\begin{aligned} f(T, x, v, y; z_1, z_2, z_3) &= \mathbb{E}^{\mathbb{Q}}[e^{z_1 x_T + z_2 v_T + z_3 y_T} | x_T = x, v_T = v, y_T = y] \\ &= e^{z_1 x + z_2 v + z_3 y}. \end{aligned}$$

## 4.2 Derivation and Solution of Pricing PDE

This section uses Itô's lemma to derive a pricing PDE using the exponential form of the joint MGF. The PDE is separated into four ODEs with known terminal conditions and closed-form solutions are obtained for each ODE.

Before obtaining a pricing PDE we must prove that the joint MGF is a martingale. The process  $\{f(t, x_t, v_t, y_t; z_1, z_2, z_3) : t \geq 0\}$  is proven to be a martingale with respect to the filtration  $\{\mathcal{F}_t : t \geq 0\}$ , associated with the Brownian motions  $\{B_t^{(1)} : t \geq 0\}$  and

$\{B_t^{(2)} : t \geq 0\}$ . Then, for any  $s < t$ , we have

$$\begin{aligned}\mathbb{E}^{\mathbb{Q}}[f(t, x_t, v_t, y_t; z_1, z_2, z_3) | \mathcal{F}_s] &= \mathbb{E}^{\mathbb{Q}}[\mathbb{E}^{\mathbb{Q}}[e^{z_1 x_T + z_2 v_T + z_3 y_T} | \mathcal{F}_t] | \mathcal{F}_s] \\ &= \mathbb{E}^{\mathbb{Q}}[e^{z_1 x_T + z_2 v_T + z_3 y_T} | \mathcal{F}_s] \\ &= f(s, x_s, v_s, y_s; z_1, z_2, z_3).\end{aligned}$$

Therefore,  $f$  is a martingale with respect to  $\{\mathcal{F}_t : t \geq 0\}$ , and a pricing PDE can be found by applying Itô's lemma and finding the expectation, which removes the Brownian motion terms from the Heston model processes and simply leaves the deterministic part, the expectation of which is equal to zero. For a review of information processes and  $\sigma$ -algebra, refer to Chapter 2.

Applying Itô's lemma for the joint MGF, we have

$$\begin{aligned}df &= \frac{\partial f}{\partial t} dt + \frac{\partial f}{\partial x} dx_t + \frac{\partial f}{\partial v} dv_t + \frac{\partial f}{\partial y} dy_t \\ &+ \frac{1}{2} \left[ \frac{\partial^2 f}{\partial x^2} \langle dx_t, dx_t \rangle + \frac{\partial^2 f}{\partial v^2} \langle dv_t, dv_t \rangle + \frac{\partial^2 f}{\partial y^2} \langle dy_t, dy_t \rangle \right. \\ &\left. + 2 \frac{\partial^2 f}{\partial x \partial v} \langle dx_t, dv_t \rangle + 2 \frac{\partial^2 f}{\partial x \partial y} \langle dx_t, dy_t \rangle + 2 \frac{\partial^2 f}{\partial v \partial y} \langle dv_t, dy_t \rangle \right].\end{aligned}$$

After making the appropriate substitutions from Equation (4.4), we get

$$\begin{aligned}df &= \frac{\partial f}{\partial t} dt + \frac{\partial f}{\partial x} \left[ (r - q - \frac{1}{2} v_t) dt + \sqrt{v_t} dB_t^{(1)} \right] + \frac{\partial f}{\partial v} \left[ \kappa(\theta - v_t) dt + \sigma \sqrt{v_t} dB_t^{(2)} \right] + \frac{\partial f}{\partial y} v_t dt \\ &+ \frac{1}{2} \left[ \frac{\partial^2 f}{\partial x^2} v_t dt + \frac{\partial^2 f}{\partial v^2} \sigma^2 v_t dt + 2 \frac{\partial^2 f}{\partial x \partial v} \rho \sigma v_t dt \right].\end{aligned}$$

Note that  $dt \times dt = dt \times dB_t^{(1)} = dt \times dB_t^{(2)} = 0$ , and therefore, some terms are omitted

above. Grouping the  $dt$  terms gives

$$df = \left[ \frac{\partial f}{\partial t} + \frac{\partial f}{\partial x} \left( r - q - \frac{1}{2} v_t \right) + \frac{\partial f}{\partial v} \kappa (\theta - v_t) + \frac{\partial f}{\partial y} v_t + \frac{1}{2} \frac{\partial^2 f}{\partial x^2} v_t + \frac{1}{2} \frac{\partial^2 f}{\partial v^2} \sigma^2 v_t + \frac{\partial^2 f}{\partial x \partial v} \rho \sigma v_t \right] dt + \frac{\partial f}{\partial x} \sqrt{v_t} dB_t^{(1)} + \frac{\partial f}{\partial v} \sigma \sqrt{v_t} dB_t^{(2)}.$$

Since  $\{f(t, x_t, v_t, y_t; z_1, z_2, z_3) : t \geq 0\}$  is a martingale,  $\mathbb{E}^Q[df] = 0$ . As mentioned previously, taking the expectation also removes the Brownian motions terms. By setting the  $dt$  term to 0, we obtain the following pricing PDE

$$\frac{\partial f}{\partial t} + \left( r - q - \frac{1}{2} v \right) \frac{\partial f}{\partial x} + \kappa (\theta - v) \frac{\partial f}{\partial v} + v \frac{\partial f}{\partial y} + \frac{1}{2} v \frac{\partial^2 f}{\partial x^2} + \frac{1}{2} \sigma^2 v \frac{\partial^2 f}{\partial v^2} + \rho \sigma v \frac{\partial^2 f}{\partial x \partial v} = 0, \quad (4.6)$$

with the terminal condition  $f(T, x, v, y; z_1, z_2, z_3) = e^{z_1 x + z_2 v + z_3 y}$ .

We assume that  $f$  has the following exponential affine form

$$f(t, x, v, y; z_1, z_2, z_3) = e^{A(t) + B(t)x + C(t)v + D(t)y}. \quad (4.7)$$

We can obtain the terminal conditions  $A(T)$ ,  $B(T)$ ,  $C(T)$  and  $D(T)$  by observing the joint MGF at time  $T$

$$f(T, x, v, y; z_1, z_2, z_3) = e^{z_1 x + z_2 v + z_3 y} = e^{A(T) + B(T)x + C(T)v + D(T)y}.$$

The conditional expectation of  $x_T$ ,  $v_T$  and  $y_T$  at time  $T$  is simply,  $x$ ,  $v$  and  $y$ , respectively. Therefore, we have  $A(T) = 0$ ,  $B(T) = z_1$ ,  $C(T) = z_2$  and  $D(T) = z_3$  as the terminal conditions.

In order to solve this PDE, we must first convert it into a set of four ODEs. The partial derivatives of  $f$  with respect to  $x$ ,  $v$  and  $y$  in (4.6) can be substituted into our

PDE (4.7) to give

$$f(A'(t) + B'(t)x + C'(t)v + D'(t)y) + (r - q - \frac{1}{2}v)fB(t) + \kappa(\theta - v)fC(t) + vfD(t) \\ + \frac{1}{2}vfB^2(t) + \frac{1}{2}\sigma^2vfC^2(t) + \rho\sigmavfB(t)C(t) = 0,$$

removing  $f$  from each term, we get

$$A'(t) + B'(t)x + C'(t)v + D'(t)y + (r - q - \frac{1}{2}v)B(t) + \kappa(\theta - v)C(t) + vD(t) \\ + \frac{1}{2}vB^2(t) + \frac{1}{2}\sigma^2vC^2(t) + \rho\sigmavB(t)C(t) = 0.$$

We may now convert our PDE into four ODEs by grouping all terms containing  $x, v, y$  and the constants and setting them equal to zero

$$\left\{ \begin{array}{l} A'(t) + (r - q)B(t) + \kappa\theta C(t) = 0, \\ B'(t) = 0, \\ C'(t) - \frac{1}{2}B(t) - \kappa C(t) + D(t) + \frac{1}{2}B^2(t) + \frac{1}{2}\sigma^2C^2(t) + \rho\sigma B(t)C(t) = 0, \\ D'(t) = 0. \end{array} \right.$$

Since  $B'(t)$  and  $D'(t)$  are equal to zero, the functions  $B(t)$  and  $D(t)$  are constants.

We know the terminal conditions of these functions and so we get

$$B(t) = z_1, \tag{4.8}$$

$$D(t) = z_3, \tag{4.9}$$

which leaves two ODEs to be solved

$$\begin{cases} A'(t) = -\kappa\theta C(t) - (r - q)z_1, \\ A(T) = 0. \end{cases} \quad (4.10)$$

$$\begin{cases} C'(t) = -\frac{1}{2}(z_1^2 - z_1 + 2z_3) - C(t)(\rho\sigma z_1 - \kappa) - \frac{1}{2}\sigma^2 C^2(t), \\ C(T) = z_2. \end{cases} \quad (4.11)$$

Equation (4.11) is recognized to be a Riccati equation and can be solved analytically using the substitution

$$C(t) = \frac{2}{\sigma^2} \frac{g'(t)}{g(t)}. \quad (4.12)$$

The purpose of this substitution is to obtain a homogeneous second order differential equation which can be solved in a straightforward manner. Finding  $C'(t)$  from Equation (4.12) and making the appropriate substitutions into Equation (4.11) gives

$$\frac{2}{\sigma^2} \frac{g''(t)g(t) - (g'(t))^2}{g^2(t)} = -\frac{1}{2}(z_1^2 - z_1 + 2z_3) - \frac{2}{\sigma^2} \frac{g'(t)}{g(t)}(\rho\sigma z_1 - \kappa) - \frac{2}{\sigma^2} \frac{(g'(t))^2}{g^2(t)}.$$

Further simplifying leads to the homogeneous second-order differential equation

$$g''(t) + (\rho\sigma z_1 - \kappa)g'(t) + \frac{\sigma^2}{4}(z_1^2 - z_1 + 2z_3)g(t) = 0. \quad (4.13)$$

We assume the general solution of  $g(t) = e^{\lambda t}$ . From this, we get  $g'(t) = \lambda e^{\lambda t}$  and  $g''(t) = \lambda^2 e^{\lambda t}$ . Substituting into (4.13) and removing  $e^{\lambda t}$  from each term gives

$$\lambda^2 + (\rho\sigma z_1 - \kappa)\lambda + \frac{\sigma^2}{4}(z_1^2 - z_1 + 2z_3) = 0.$$

Solving for  $\lambda$  yields

$$\lambda_{1,2} = \frac{-(\rho\sigma z_1 - \kappa) \pm \sqrt{\Delta}}{2}, \quad (4.14)$$

where

$$\Delta = (\rho\sigma z_1 - \kappa)^2 - \sigma^2(z_1^2 - z_1 + 2z_3).$$

The general solution of  $g(t)$  is

$$g(t) = c_1 e^{\lambda_1 t} + c_2 e^{\lambda_2 t},$$

therefore,  $C(t)$  can then be written in terms of  $\lambda_1$  and  $\lambda_2$  as

$$C(t) = \frac{2}{\sigma^2} \frac{\lambda_1 c_1 e^{\lambda_1 t} + \lambda_2 c_2 e^{\lambda_2 t}}{c_1 e^{\lambda_1 t} + c_2 e^{\lambda_2 t}}.$$

To remove the unknown coefficients  $c_1$  and  $c_2$  from  $C(t)$ , we find the ratio  $\frac{c_1}{c_2}$ , which is denoted by  $\omega$ . But first we must apply the boundary condition  $C(T) = z_2$ , then we have

$$\omega := \frac{c_1}{c_2} = \frac{e^{\lambda_2 T} (\sigma^2 z_2 - 2\lambda_2)}{e^{\lambda_1 T} (2\lambda_1 - \sigma^2 z_2)}.$$

We obtain the analytical solution for  $C(t)$  by dividing the numerator and denominator by  $c_2$  and using the ratio  $\omega$

$$C(t) = \frac{2}{\sigma^2} \frac{\lambda_1 c_1 e^{\lambda_1 t} + \lambda_2 c_2 e^{\lambda_2 t}}{c_1 e^{\lambda_1 t} + c_2 e^{\lambda_2 t}} = \frac{2}{\sigma^2} \frac{\lambda_1 \omega e^{\lambda_1 t} + \lambda_2 e^{\lambda_2 t}}{\omega e^{\lambda_1 t} + e^{\lambda_2 t}}. \quad (4.15)$$

The solution to  $A(t)$  is found by substituting  $C(t)$  from (4.12) into (4.10) and integrating

with respect to  $t$  from  $t$  to  $T$

$$A(T) - A(t) = -\frac{2\kappa\theta}{\sigma^2} \ln\left(\frac{g(T)}{g(t)}\right) - (r - q)z_1(T - t).$$

By applying the terminal condition  $A(T) = 0$ , we can remove  $A(T)$ . Furthermore, plugging in the general solution of  $g(t)$  and  $g(T)$  and simplifying leads to the closed-form solution for  $A(t)$

$$\begin{aligned} A(t) &= \frac{2\kappa\theta}{\sigma^2} \ln\left(\frac{g(T)}{g(t)}\right) + (r - q)z_1(T - t) \\ &= \frac{2\kappa\theta}{\sigma^2} \ln\left(\frac{c_1 e^{\lambda_1 T} + c_2 e^{\lambda_2 T}}{c_1 e^{\lambda_1 t} + c_2 e^{\lambda_2 t}}\right) + (r - q)z_1(T - t) \\ &= \frac{2\kappa\theta}{\sigma^2} \ln\left(\frac{\omega e^{\lambda_1 T} + e^{\lambda_2 T}}{\omega e^{\lambda_1 t} + e^{\lambda_2 t}}\right) + (r - q)z_1(T - t). \end{aligned} \quad (4.16)$$

The following proposition summarizes the derivations from this section.

**Proposition 4.2.1.** (Moment generating function). Given a pricing PDE of the form

$$\frac{\partial f}{\partial t} + (r - q - \frac{1}{2}v)\frac{\partial f}{\partial x} + \kappa(\theta - v)\frac{\partial f}{\partial v} + v\frac{\partial f}{\partial y} + \frac{1}{2}v\frac{\partial^2 f}{\partial x^2} + \frac{1}{2}\sigma^2 v\frac{\partial^2 f}{\partial v^2} + \rho\sigma v\frac{\partial^2 f}{\partial x\partial v} = 0.$$

where  $f(t, x, v, y; z_1, z_2, z_3)$  represents the joint MGF and has the form

$$f(t, x, v, y; z_1, z_2, z_3) = e^{A(t)+B(t)x+C(t)v+D(t)y},$$

the closed-form solutions for  $A(t)$ ,  $B(t)$ ,  $C(t)$  and  $D(t)$  are derived as

$$\left\{ \begin{array}{l} A(t) = \frac{2\kappa\theta}{\sigma^2} \ln \left( \frac{\omega e^{\lambda_1 T} + e^{\lambda_2 T}}{\omega e^{\lambda_1 t} + e^{\lambda_2 t}} \right) + (r - q)z_1(T - t), \\ B(t) = z_1, \\ C(t) = \frac{2}{\sigma^2} \frac{\lambda_1 \omega e^{\lambda_1 t} + \lambda_2 e^{\lambda_2 t}}{\omega e^{\lambda_1 t} + e^{\lambda_2 t}}, \\ D(t) = z_3. \end{array} \right.$$

### 4.3 Option Pricing

In this section, we introduce a link between the joint MGF  $f(t, x, v, y; z_1, z_2, z_3)$  and the characteristic function of an LETF. This link is necessary to provide an analytical solution for the call price of an LETF. Once the characteristic function is defined, the Carr-Madan Fourier transform method [6] is used to derive the final call price function. The Carr-Madan approach introduces a modified call price function with a dampening factor  $\alpha$  in order to make the call price function square-integrable.

#### 4.3.1 LETF Characteristic Function

As mentioned in Chapter 3, the price dynamics of an LETF is linked to its reference index by

$$\frac{dL_t}{L_t} = \beta \frac{dS_t}{S_t} + (1 - \beta)r dt, \quad (4.17)$$

where  $L_t$  is the LETF price,  $S_t$  is the underlying index price and  $\beta$  is the LETF leverage ratio.

As we proved in Chapter 3, using Itô's lemma,  $L_t$  can be expressed in terms of  $S_t$

as follows

$$\ln\left(\frac{L_t}{L_0}\right) = \beta \ln\left(\frac{S_t}{S_0}\right) + \frac{\beta - \beta^2}{2} \int_0^t v_u du + (1 - \beta)rt,$$

or, equivalently

$$\ln L_t = \ln L_0 + \beta \ln\left(\frac{S_t}{S_0}\right) + \frac{\beta - \beta^2}{2} \int_0^t v_u du + (1 - \beta)rt. \quad (4.18)$$

Note that, unlike in Chapter 3, the expense ratio  $f$  has been omitted from Equation (4.18) for the purpose of simplicity. The expense ratio can be added later for specific cases if necessary.

We denote  $l_t = \ln L_t$  and use  $x_t = \ln S_t$  and  $y_t = \int_0^t v_u du$ , and rewrite Equation (4.18) at time  $T$  as

$$L_T = e^{\beta x_T + \frac{\beta - \beta^2}{2} y_T + l_0 - \beta x_0 + (1 - \beta)rT}. \quad (4.19)$$

Then the characteristic function of  $l_t$  can be written in the form

$$\begin{aligned} \phi_0(u) &= \mathbb{E}_0^{\mathbb{Q}} \left[ e^{iul_T} \right] = \mathbb{E}_0^{\mathbb{Q}} \left[ e^{iu(l_0 + \beta(x_T - x_0) + \frac{\beta - \beta^2}{2} \int_0^T v_u du + (1 - \beta)rT)} \right] \\ &= \mathbb{E}_0^{\mathbb{Q}} \left[ e^{iu(l_0 - \beta x_0 + (1 - \beta)rT)} e^{iu\beta x_T + iu\frac{\beta - \beta^2}{2} \int_0^T v_u du} \right]. \end{aligned} \quad (4.20)$$

Since  $\mathbb{E}_0^{\mathbb{Q}} \left[ e^{iu(l_0 - \beta x_0 + (1 - \beta)rT)} \right] = e^{iu(l_0 - \beta x_0 + (1 - \beta)rT)}$ , we can take this term outside the expectation. The remaining term inside the expectation is simply the joint MGF from Equation (4.5) with the coefficients  $z_1$  and  $z_3$  defined in terms of  $i, u$  and  $\beta$  and  $z_2 = 0$ .

We can then rewrite the characteristic function of  $l_t$  in terms of the joint MGF

$$\phi_0(u) = e^{iu(l_0 - \beta x_0 + (1 - \beta)rT)} f\left(0, x, v, y; iu\beta, 0, iu\frac{\beta - \beta^2}{2}\right). \quad (4.21)$$

### 4.3.2 Carr-Madan Fourier Transform Method

First, we determine the theoretical call price of an LETF as the discounted expectation of the payoff at maturity time. Using Equation (4.19), we can rewrite this call price as a function of the two processes,  $x_T$  and  $y_T$ . Denoting,  $C_0$  as the price of a European call option at time 0 and  $K$  as the strike price, we obtain the call price at time 0 as

$$\begin{aligned} C_0(K) &= \mathbb{E}_0^{\mathbb{Q}} \left[ e^{-rT} (L_T - K)^+ \right] = \mathbb{E}_0^{\mathbb{Q}} \left[ e^{-rT} \left( e^{\beta x_T + \frac{\beta - \beta^2}{2} y_T + l_0 - \beta x_0 + (1 - \beta)rT} - K \right)^+ \right] \\ &= \mathbb{E}_0^{\mathbb{Q}} \left[ e^{a(T)} \left( e^{d_1 x_T + d_2 y_T} - K' \right)^+ \right], \end{aligned} \quad (4.22)$$

where  $a(T) = l_0 - \beta x_0 - \beta rT$ ,  $K' = K e^{-(l_0 - \beta x_0 + (1 - \beta)rT)}$ ,  $d_1 = \beta$ ,  $d_2 = \frac{\beta - \beta^2}{2}$ . Since  $a(T)$  is a constant, we can move it outside the expectation parentheses.

Denoting  $k = \ln K'$ , we can then rewrite the call price function as the joint cumulative distribution function of  $x$  and  $y$

$$\begin{aligned} C_0(k) &= \mathbb{E}_0^{\mathbb{Q}} \left[ e^{a(T)} \left( e^{d_1 x_T + d_2 y_T} - e^k \right)^+ \right] \\ &= e^{a(T)} \int_{-\infty}^{\infty} \int_{-\infty}^{\infty} \left( e^{d_1 x + d_2 y} - e^k \right)^+ dF(x, y). \end{aligned} \quad (4.23)$$

At this point, we would have to evaluate the call price integral from  $-\infty$  to  $d_1 x + d_2 y$ , since that is the range for the call option to be exercised. But this call price function is not square-integrable and therefore we will not be able to obtain an analytical solution. Instead, we introduce a modified call price  $c_0(k)$  using a dampening factor  $\alpha$

$$c_0(k) = e^{\alpha k} C_0(k). \quad (4.24)$$

As we will see later,  $\alpha$  must be strictly positive for the call price function to be square-integrable.

With the introduction of Equation (4.24), we denote  $\mathfrak{F}_c(z)$  the Fourier transform

of the modified call price. We substitute Equations (4.23) and (4.24) into the Fourier transform function to evaluate it in terms of our modified call price

$$\begin{aligned}
\mathfrak{F}_c(z) &= \int_{-\infty}^{\infty} e^{izk} c_0(k) dk \\
&= \int_{-\infty}^{\infty} e^{izk} e^{\alpha k} C_0(k) dk \\
&= \int_{-\infty}^{\infty} e^{(iz+\alpha)k} \left[ e^{a(T)} \int_{-\infty}^{\infty} \int_{-\infty}^{\infty} (e^{d_1x+d_2y} - e^k)^+ dF(x, y) \right] dk \\
&= e^{a(T)} \int_{-\infty}^{\infty} \int_{-\infty}^{\infty} \left[ \int_{-\infty}^{\infty} e^{(iz+\alpha)k} (e^{d_1x+d_2y} - e^k)^+ dk \right] dF(x, y) \\
&= e^{a(T)} \int_{-\infty}^{\infty} \int_{-\infty}^{\infty} \left[ \int_{-\infty}^{d_1x+d_2y} e^{(iz+\alpha)k} (e^{d_1x+d_2y} - e^k) dk \right] dF(x, y) \\
&= e^{a(T)} \int_{-\infty}^{\infty} \int_{-\infty}^{\infty} \left[ \int_{-\infty}^{d_1x+d_2y} (e^{d_1x+d_2y} e^{(iz+\alpha)k} - e^{(iz+\alpha+1)k}) dk \right] dF(x, y) \\
&= e^{a(T)} \int_{-\infty}^{\infty} \int_{-\infty}^{\infty} \left[ \frac{e^{d_1x+d_2y} e^{(iz+\alpha)k}}{(iz+\alpha)} - \frac{e^{(iz+\alpha+1)k}}{(iz+\alpha+1)} \Big|_{-\infty}^{d_1x+d_2y} \right] dF(x, y). \quad (4.25)
\end{aligned}$$

As mentioned earlier, we choose an  $\alpha > 0$  in order to evaluate the integral and we get  $e^{-(iz+\alpha)\infty} = 0$  and  $e^{-(iz+\alpha+1)\infty} = 0$ . Further simplification allows us to write the Fourier transform in terms of our joint MGF, which is known analytically

$$\begin{aligned}
\mathfrak{F}_c(z) &= e^{a(T)} \int_{-\infty}^{\infty} \int_{-\infty}^{\infty} \left[ \frac{e^{d_1x+d_2y} e^{(iz+\alpha)(d_1x+d_2y)}}{(iz+\alpha)} - \frac{e^{(iz+\alpha+1)(d_1x+d_2y)}}{(iz+\alpha+1)} \right] dF(x, y) \\
&= e^{a(T)} \int_{-\infty}^{\infty} \int_{-\infty}^{\infty} \left[ \frac{e^{(iz+\alpha+1)(d_1x+d_2y)}}{(iz+\alpha)} - \frac{e^{(iz+\alpha+1)(d_1x+d_2y)}}{(iz+\alpha+1)} \right] dF(x, y) \\
&= e^{a(T)} \int_{-\infty}^{\infty} \int_{-\infty}^{\infty} \frac{e^{(iz+\alpha+1)(d_1x+d_2y)}}{(iz+\alpha)(iz+\alpha+1)} dF(x, y) \\
&= e^{a(T)} \int_{-\infty}^{\infty} \int_{-\infty}^{\infty} \frac{e^{i(z-i\alpha-i)d_1x+i(z-i\alpha-i)d_2y}}{(iz+\alpha)(iz+\alpha+1)} dF(x, y) \\
&= \frac{e^{a(T)}}{(iz+\alpha)(iz+\alpha+1)} f(0, x, v, y; i(z-i\alpha-i)d_1, 0, i(z-i\alpha-i)d_2). \quad (4.26)
\end{aligned}$$

By applying the inverse Fourier transform to the second equality in Equation (4.25), we can evaluate our call price  $C_0(k)$  in terms of the Fourier transform  $\mathfrak{F}_c(z)$ , and

therefore our joint MGF

$$\begin{aligned}
C_0(k) &= \frac{1}{2\pi} \int_{-\infty}^{\infty} e^{-izk} e^{-\alpha k} \mathfrak{F}_c(z) dz \\
&= \frac{e^{a(T)}}{2\pi} \int_{-\infty}^{\infty} \frac{e^{-(iz+\alpha)k} f(0, x, v, y; i(z-i\alpha-i)d_1, 0, i(z-i\alpha-i)d_2)}{(iz+\alpha)(iz+\alpha+1)} dz \\
&= \frac{e^{a(T)}}{\pi} \int_0^{\infty} \frac{e^{-(iz+\alpha)k} f(0, x, v, y; (iz+\alpha+1)d_1, 0, (iz+\alpha+1)d_2)}{(iz+\alpha)(iz+\alpha+1)} dz,
\end{aligned}$$

where

$$\begin{aligned}
f(0, x, v, y; (iz+\alpha+1)d_1, 0, (iz+\alpha+1)d_2) &= e^{A(0; z_1, z_2, z_3) + (iz+\alpha+1)d_1 x_0 + C(0; z_1, z_2, z_3) v_0}, \\
d_1 = \beta, \quad d_2 = \frac{\beta - \beta^2}{2}, \quad z_1 = (iz+\alpha+1)\beta, \quad z_2 = 0, \quad z_3 = (iz+\alpha+1)\frac{\beta - \beta^2}{2},
\end{aligned}$$

and the exact solutions of  $A(0; z_1, z_2, z_3)$  and  $C(0; z_1, z_2, z_3)$  are found in Section 4.2.1.

Note that the  $y$  term is disregarded since  $y_0 = 0$ .

Finally, we make the following substitutions to evaluate our call price function

$$\left\{ \begin{array}{l} a(T) = l_0 - \beta x_0 - \beta rT, \\ k = \ln K' = \ln K - a(T) - rT, \\ l_0 = \ln L_0, \end{array} \right.$$

and simplify to get

$$\begin{aligned}
C_0(K) &= \frac{1}{\pi} \int_0^{\infty} \frac{e^{-(iz+\alpha)(\ln K - rT)} e^{(iz+\alpha+1)(l_0 - \beta x_0 - \beta rT)} e^{A(0; z_1, z_2, z_3) + (iz+\alpha+1)\beta x_0 + C(0; z_1, z_2, z_3) v_0}}{(iz+\alpha)(iz+\alpha+1)} dz \\
&= \frac{1}{\pi} \int_0^{\infty} \frac{e^{-(iz+\alpha)(\ln K - rT)} e^{(iz+\alpha+1)(\ln L_0 - \beta rT)} e^{A(0; z_1, z_2, z_3) + C(0; z_1, z_2, z_3) v_0}}{(iz+\alpha)(iz+\alpha+1)} dz \\
&= \frac{1}{\pi} \int_0^{\infty} \frac{e^{(iz+\alpha+1)(\ln L_0 - \beta rT) - (iz+\alpha)(\ln K - rT) + A(0; z_1, z_2, z_3) + C(0; z_1, z_2, z_3) v_0}}{(iz+\alpha)(iz+\alpha+1)} dz.
\end{aligned} \tag{4.27}$$

Notice from Equation (4.27) that the call price is a function of  $L_0$ , the LETF price at time 0, and  $v_0$ , the variance of the underlying index at time 0. It is not dependent on the underlying index value,  $S_0$ .

The following proposition summarizes the findings from this section.

**Proposition 4.3.1.** (Option pricing formula). Given the LETF dynamics in Equation (4.19), the price of a European call option on an LETF, based on the Carr-Madan Fourier transform method is given by

$$C_0(K) = \frac{1}{\pi} \int_0^\infty \frac{e^{(iz+\alpha+1)(\ln L_0 - \beta r T) - (iz+\alpha)(\ln K - r T) + A(0; z_1, z_2, z_3) + C(0; z_1, z_2, z_3)v_0}}{(iz + \alpha)(iz + \alpha + 1)} dz, \quad (4.28)$$

where

$$A(0; z_1, z_2, z_3) = \frac{2\kappa\theta}{\sigma^2} \ln \left( \frac{\omega e^{\lambda_1 T} + e^{\lambda_2 T}}{\omega + 1} \right) + (r - q)z_1 T,$$

$$C(0; z_1, z_2, z_3) = \frac{2}{\sigma^2} \left( \frac{\lambda_1 \omega + \lambda_2}{\omega + 1} \right),$$

$$\omega = \frac{e^{\lambda_2 T}(\sigma^2 z_2 - 2\lambda_2)}{e^{\lambda_1 T}(2\lambda_1 - \sigma^2 z_2)},$$

$$\lambda_{1,2} = \frac{-(\rho\sigma z_1 - \kappa) \pm \sqrt{\Delta}}{2},$$

$$\Delta = (\rho\sigma z_1 - \kappa)^2 - \sigma^2(z_1^2 - z_1 + 2z_3),$$

$$z_1 = (iz + \alpha + 1)\beta, \quad z_2 = 0, \quad z_3 = (iz + \alpha + 1)\frac{\beta - \beta^2}{2}.$$

# Chapter 5

## Numerical Analysis

This chapter is split into two sections with different purposes. Section 5.1 compares the call prices obtained from the pricing formula in Equation (4.28) to the call prices generated from Monte-Carlo simulations for different leverage ratios. The Monte Carlo simulations of LETFs are generated using the Euler discretization of the Heston model to acquire values for  $S_t$ , and then applying Equation (4.19) to obtain values for  $L_t$ . The comparison is illustrated in terms of the relative percentage error between the results. This section also computes call prices with respect to different time-to-maturity and moneyness levels and compares the values with those obtained from Monte Carlo simulations.

Section 5.2 performs sensitivity analysis on the Heston model parameters. The sensitivity analysis displays the change in call price with varying parameters and justifies the robustness of our option pricing model in terms of its ability to provide reasonable call prices under extreme parametric conditions.

## 5.1 Analysis of Option Pricing Formula

This section attempts to test the accuracy of our option pricing formula from Equation (4.28). The at-the-money call price obtained from our formula is compared to Monte Carlo simulations. To be able to simulate option prices, the Heston model in Equation (4.1) must first be discretized to solve for  $S_t$  at each time point from  $t = 0$  to  $T$ , where  $T$  is the time to maturity, through which we can determine the LEFT price  $L_t$  using Equation (4.19). The discretization is achieved using the Euler scheme which gives

$$\begin{aligned} S_{t+\Delta} &= S_t + (r - q)S_t\Delta + \sqrt{v_t\Delta} S_t Z_S, \\ v_{t+\Delta} &= \kappa(\theta - v_t)\Delta + \sigma\sqrt{v_t\Delta} Z_v, \end{aligned} \quad (5.1)$$

where  $Z_S$  and  $Z_v$  are standard normal variables with correlation  $\rho$  and can be computed as

$$\begin{aligned} Z_v &= \Phi^{-1}(z_1), \\ Z_S &= \rho Z_v + \sqrt{1 - \rho^2}\Phi^{-1}(z_2), \end{aligned}$$

where  $\Phi^{-1}$  is the inverse cumulative normal distribution function,  $z_1$  and  $z_2$  are independent uniform samples in the interval  $(0, 1)$ , and  $\Delta$  is taken as  $\frac{1}{252}$  or 1-day increments from time 0 to maturity date.

A problem with this discretization of  $v_t$  is the possibility of  $v_t$  to have a negative value. An easy fix that provides minimal discretization bias is to apply a constraint  $v_t^+ = \max(v_t, 0)$

$$\begin{aligned} S_{t+\Delta} &= S_t + (r - q)S_t\Delta + \sqrt{v_t^+\Delta} S_t Z_S, \\ v_{t+\Delta} &= \kappa(\theta - v_t^+)\Delta + \sigma\sqrt{v_t^+\Delta} Z_v, \end{aligned} \quad (5.2)$$

Essentially this process creates a sample path for the underlying index price from

$t = 0$  to maturity date. Using this dataset, the LETF price can also be simulated using Equation (4.19)

$$L_t = e^{\ln L_0 + \beta \ln \frac{S_t}{S_0} + \frac{\beta - \beta^2}{2} \int_0^t v_u du + (1 - \beta)rt}.$$

After gathering a sample path for  $L_t$ , the simulated call price is obtained as

$$\hat{C}(T) = e^{-rT} (L_T - K)^+.$$

Running multiple simulations and finding the mean call price gives us an estimate of the call price of an LETF, which is then compared with the result obtained by using our model.

The parameter values obtained from [2], are as follows

$\kappa$	$\theta$	$\sigma$	$\rho$	$\alpha$	$v_0$	$r$
5.07	0.0457	0.48	-0.767	1.5	0.25	0.05

Table 5.1: Parameter values used to generate call option prices.

We take  $S_0 = L_0 = 100$ , and since we are considering ATM options,  $K = 100$ . The time to maturity  $T$  is taken as 0.25 or approximately 90 days. This section looks at LETF  $\beta$  values from  $-3$  to  $3$ . The Monte Carlo simulation creates a 90-day sample path for the underlying index and the LETF, which is then simulated 1,000, 10,000 and 100,000 times and compared with the results from our option pricing model.

Figures 5.1 and 5.2 show possible sample paths generated from Monte Carlo simulations of an LETF price process for  $\beta$  values of 2 and 3, respectively. The simulations are generated using the parameter values from Table 5.1. Note that the three sample paths in each figure do not differ in parameters and only deviate from each other due to the presence of Brownian motion in the Heston model. The sample paths illustrated in both figures are not correlated in any way and have different underlying index values,

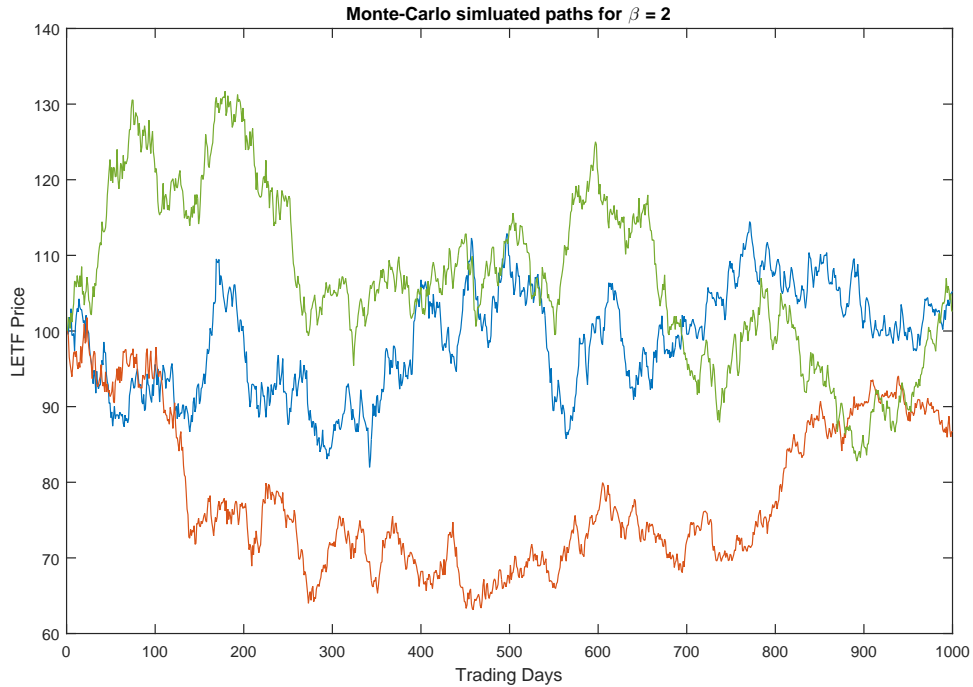


Figure 5.1: Three sample paths of an ETF with  $\beta = 2$  generated using Monte Carlo Simulations for 1000 trading days.

although  $S_0 = 100$  in both scenarios. As you would expect, the paths for  $\beta = 3$  show larger exaggeration in price changes. In Figure 5.1, the lowest price level reached is approximately \$65 and the highest is about \$130. On the other hand, prices in Figure 5.2 almost reach a high of \$160 and a low of \$20.

Table 5.2 displays the call option prices determined by our model for different values of  $\beta$  and also the Monte Carlo simulation with varying number of paths. The table also lists the computation time, given in seconds, for the different number of simulations and  $\beta$  values, and the relative percentage error,  $\eta$ , which is defined as

$$\eta = 100\% \times \frac{|\text{Call}_{Model} - \text{Call}_{MC}|}{\text{Call}_{Model}}. \quad (5.3)$$

Looking at the model prices, we can see the call prices for ETFs with the same absolute  $\beta$  values are similar, although bearish ETFs have a higher call price than

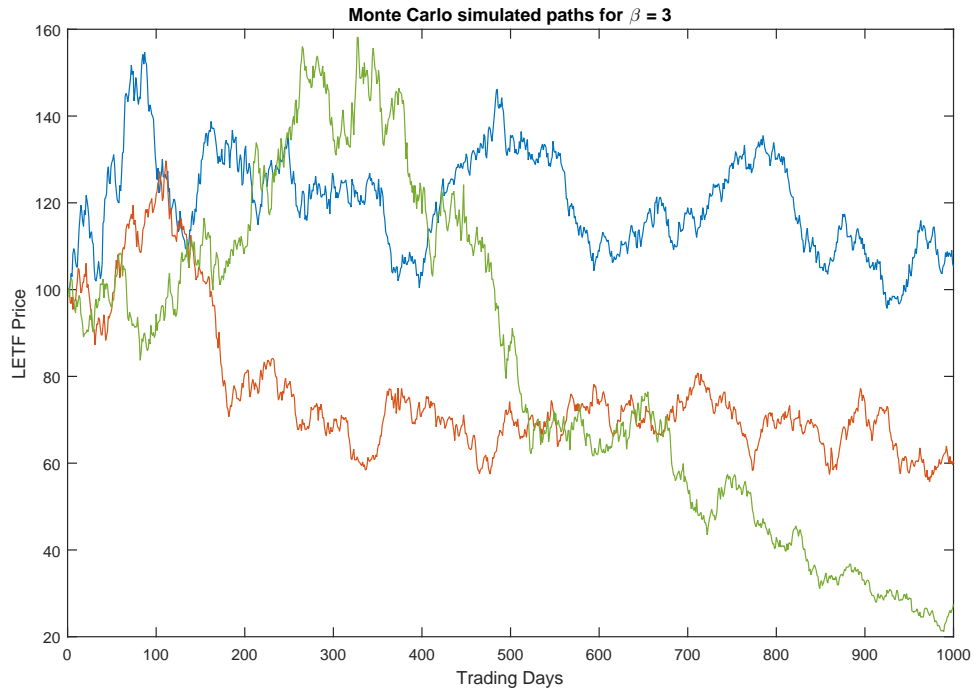


Figure 5.2: Three sample paths of an LETF with  $\beta = 3$  generated using Monte Carlo Simulations for 1000 trading days.

	Leverage Ratio				
	2	3	-1	-2	-3
$Call_{Model}$	16.107	23.444	8.554	16.566	24.555
$Call_{1,000}$	16.673	23.948	9.276	18.069	21.871
Time	3.041	3.025	3.120	3.188	3.120
$\eta$ (%)	3.512	2.150	8.440	9.073	10.931
$Call_{10,000}$	16.316	23.305	8.581	16.982	26.4899
Time	29.843	30.309	29.990	30.109	30.596
$\eta$ (%)	1.298	0.593	0.316	2.511	7.880
$Call_{100,000}$	15.905	23.422	8.531	16.796	24.8181
Time	308.194	299.398	310.861	306.781	301.493
$\eta$ (%)	1.254	0.094	0.269	1.388	1.071

Table 5.2: ATM call option prices from model and Monte Carlo simulations with 1,000, 10,000 and 100,000 paths.

their bullish counterpart, possibly due to the larger volatility decay which adds to the uncertainty of its price at maturity time. The  $Call_{100,000}$  prices provide results accurate to the model, with the highest error being only 1.388% for  $\beta = -2$ . The average error

for 1,000 simulated paths is 6.821%, for 10,000 paths is 2.520% and for 100,000 paths is 0.815%. In general, the Monte Carlo simulated prices show higher deviations from the model for bearish LETFs. For 1,000 paths, the average error for bullish LETFs is 2.831% and for bearish LETFs is 9.481%. For 10,000 paths, the average error is 0.946% and 3.569% for bullish and bearish LETFs, respectively. Finally, in the case of 100,000 paths, the average error is 0.674% and 0.909%, for bullish and bearish LETFs, respectively. Comparing the call prices from our model with those of Monte Carlo simulations, we are able to justify the use of our model for pricing ATM call options for LETFs.

The table shows that the relationship between the computational time and the number of simulated paths is approximately linear. The average computational time for 1,000 paths is 3.099s, for 10,000 paths is 30.169s, and for 100,000 paths is 305.345s. With an increase in the number of simulations, the simulated call prices converge to the prices from our option pricing formula, since the error is decreasing. Therefore, our option pricing formula provides an accurate result without the large computational times of running simulations and is therefore a better alternative to the Monte Carlo method.

### 5.1.1 Varying Time-to-Maturity

This section analyzes our option pricing formula with varying time-to-maturity levels,  $T$ , from 0 to 1. As mentioned earlier,  $T$  is specified in terms of years. Observing the simulation results from Table 5.2, we see that  $\text{Call}_{10,000}$  and  $\text{Call}_{100,000}$  provide similar results but with the latter having around ten times larger computational times. In this regard, the  $\text{Call}_{10,000}$  values are preferred. But for the sake of accuracy, we perform further analysis using the  $\text{Call}_{100,000}$  values.

The prices obtained from our formula are compared with results from Monte Carlo simulations of 100,000 paths. The results are summarized in Table 5.3. The table

shows an increase in call prices for higher values of  $T$ , as expected. The error between  $\text{Call}_{Model}$  and  $\text{Call}_{MC}$ , calculated from Equation (5.3), is fairly acceptable, and it is observed that bearish LETFs have a larger error in most cases. From the table, we also observe that the average error amongst all the leverage ratios increases for higher values of  $T$ . The maximum error observed was 4.630% for an LETF with a leverage ratio of -1 and a time-to-maturity of 1 year.

Table 5.3 also shows the computational time for each value of  $T$  as an average amongst the leverage ratios. The computational times vary with  $T$  because  $T$  dictates the number of days that are simulated to create a single path, which is then replicated 100,000 times. Therefore, the computational times will increase with larger  $T$  values. We can see from the table that the relationship between computational times and  $T$  values is linear, although a line plot provides a better visual representation as we see later in this section.

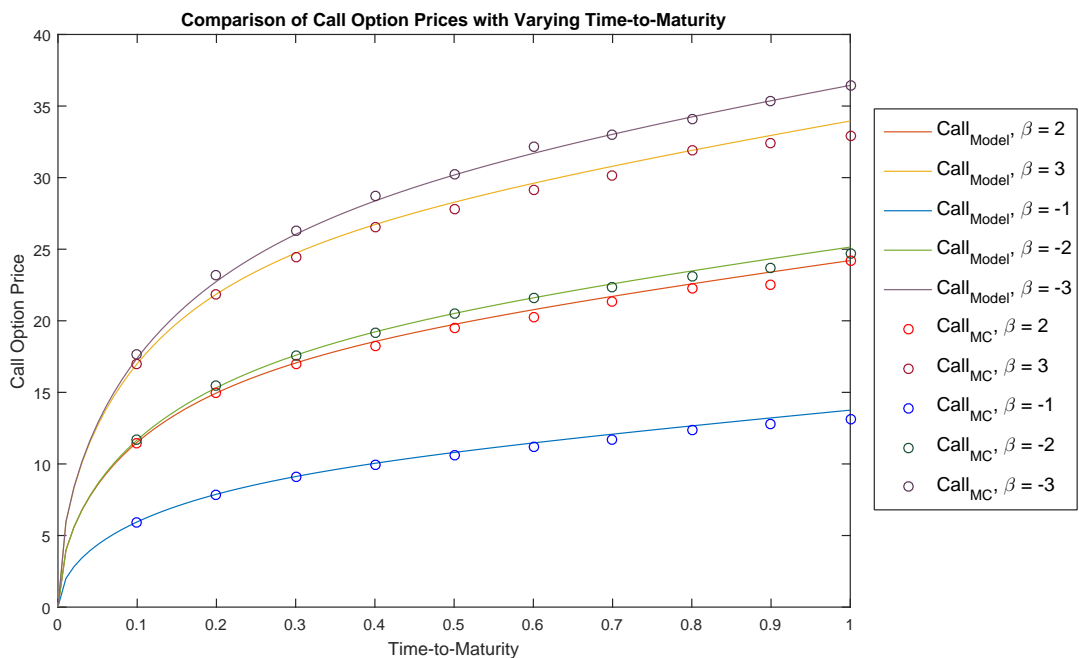


Figure 5.3: Comparison of error between  $\text{Call}_{Model}$  and  $\text{Call}_{MC}$  with varying time-to-maturity.

T		Leverage Ratio					Average Time
		2	3	-1	-2	-3	
0.1	Call <sub>Model</sub>	11.516	17.002	5.953	11.680	17.396	110.101
	Call <sub>MC</sub>	11.445	17.012	5.897	11.716	17.653	
	$\eta$ (%)	0.617	0.059	0.941	0.308	1.477	
0.2	Call <sub>Model</sub>	14.957	21.862	7.881	15.325	22.749	226.376
	Call <sub>MC</sub>	14.930	21.884	7.824	15.441	23.166	
	$\eta$ (%)	0.181	0.101	0.723	0.757	1.833	
0.3	Call <sub>Model</sub>	17.051	24.722	9.119	17.590	26.036	348.743
	Call <sub>MC</sub>	16.957	24.413	9.091	17.604	26.257	
	$\eta$ (%)	0.551	1.250	0.307	0.080	0.849	
0.4	Call <sub>Model</sub>	18.549	26.716	10.043	19.219	28.366	459.227
	Call <sub>MC</sub>	18.254	26.551	9.970	19.202	28.689	
	$\eta$ (%)	1.590	0.618	0.727	0.088	1.139	
0.5	Call <sub>Model</sub>	19.745	28.277	10.801	20.507	30.180	580.963
	Call <sub>MC</sub>	19.509	27.835	10.593	20.496	30.233	
	$\eta$ (%)	1.195	1.563	1.926	0.054	0.176	
0.6	Call <sub>Model</sub>	20.774	29.603	11.468	21.601	31.694	694.373
	Call <sub>MC</sub>	20.275	29.144	11.188	21.581	32.181	
	$\eta$ (%)	2.402	1.551	2.442	0.093	1.537	
0.7	Call <sub>Model</sub>	21.706	30.794	12.080	22.578	33.025	819.753
	Call <sub>MC</sub>	21.359	30.116	11.713	22.338	33.021	
	$\eta$ (%)	1.599	2.202	3.038	1.063	0.012	
0.8	Call <sub>Model</sub>	22.577	31.900	12.659	23.480	34.239	928.190
	Call <sub>MC</sub>	22.261	31.933	12.384	23.122	34.084	
	$\eta$ (%)	1.400	0.103	2.172	1.525	0.453	
0.9	Call <sub>Model</sub>	23.407	32.949	13.216	24.332	35.371	1010.237
	Call <sub>MC</sub>	22.554	32.430	12.787	23.667	35.324	
	$\eta$ (%)	3.644	1.575	3.246	2.733	0.133	
1	Call <sub>Model</sub>	24.206	33.954	13.758	25.149	36.445	1147.744
	Call <sub>MC</sub>	24.578	32.924	13.121	24.721	36.450	
	$\eta$ (%)	1.537	3.034	4.630	1.702	0.014	

Table 5.3: Call prices generated from model and Monte Carlo simulations for various time-to-maturity levels.

Figure 5.3 illustrates the call price data from Table 5.3 for the various leverage ratios. This figure provides a better visual representation of the error between Call<sub>Model</sub> and Call<sub>MC</sub>. We can see from the figure that this error is negligible in most cases and is usually higher for larger  $T$  values, as was mentioned earlier. In regards to the sensitivity of call prices with respect to  $T$ , we observe that the call prices are more sensitive to

change with lower  $T$  values.

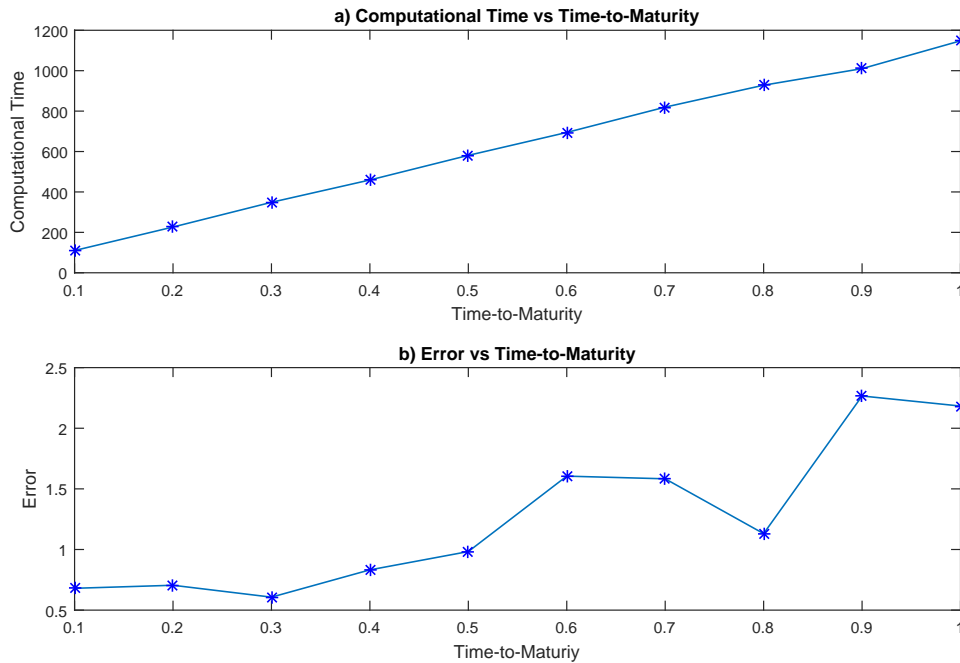


Figure 5.4: Change in computational time and  $\eta$  with time-to-maturity.

Finally, Figures 5.4a and 5.4b present the computational time and the error in call prices for different values of  $T$ . From Figure 5.4a we can see that the computational time and time-to-maturity have an approximately linear relationship, with slight deviation when  $T = 0.9$ . This linearity is to be expected, since the calculations do not change and only the number of simulations are increased. In Figure 5.4b we can see that the error between  $\text{Call}_{Model}$  and  $\text{Call}_{MC}$  is roughly increasing with higher values of  $T$ . A possible reason for this could be the fact that larger  $T$  values simulate more daily prices for a single path. For example,  $T = 0.25$  simulates a 3-month sample path, whereas for  $T = 1$ , a 1-year sample path is simulated. The longer path could imply more randomness at each time step which would accumulate and cause a larger error over time.

### 5.1.2 Varying Moneyness

We now examine the sensitivity of call prices from our model to changes in moneyness. The simple moneyness scale is defined as  $M = \frac{L_0}{K}$ , where  $L_0$  is the initial spot price of an LETF and with  $M = 1$  being an at-the-money (ATM) call option,  $M > 1$  being an in-the-money (ITM) call option, and  $M < 1$  an out-of-the-money (OTM) call option. Note that we are working with initial spot prices rather than the price at maturity time and therefore the moneyness levels are at time 0. ITM implies the call option will be exercised at maturity, and if a call option is OTM on the maturity date, it will not be exercised. We choose specific moneyness levels between 0.85 and 1.15 and vary the strike price  $K$ , while holding  $L_0$  constant at 100.

Table 5.4 presents the call prices from our model and Monte Carlo simulations for different moneyness levels and  $\beta$  values. As with prior analysis, the MC call prices consists of 100,000 sample paths. We re-introduce the relative percentage error  $\eta$  from Equation (5.3). The table shows that the  $\eta$  values are consistently low in most cases with no significant pattern in errors. Overall, the  $\text{Call}_{\text{Model}}$  and  $\text{Call}_{\text{MC}}$  are relatively similar and we can conclude that our model is consistent with varying moneyness.

Figure 5.5 provides a better visual representation of the call prices from Table 5.4. From the figure we can see that call prices within our range of moneyness seem to be linear with moneyness for all leverage ratios except  $\beta = -1$ . Another important note is that, at a certain moneyness level when the call option is ITM, the  $\beta = -2$  call prices intersect with  $\beta = 2$  call prices and become lower than the latter. If we expanded our range of moneyness, we would see that the same effect applies to  $\beta = 3$  and  $-3$ .

Moneyness		Leverage Ratio				
		2	3	-1	-2	-3
0.85	Call <sub>Model</sub>	9.369	16.940	3.277	10.957	19.249
	Call <sub>MC</sub>	9.264	16.838	3.299	11.001	19.424
	$\eta$ (%)	1.121	0.602	0.671	0.402	0.909
0.90	Call <sub>Model</sub>	11.543	19.138	4.712	12.754	21.029
	Call <sub>MC</sub>	11.407	19.102	4.701	12.903	21.349
	$\eta$ (%)	1.178	0.188	0.233	1.168	1.522
0.95	Call <sub>Model</sub>	13.802	21.311	6.477	14.630	22.800
	Call <sub>MC</sub>	13.594	21.179	6.406	14.650	22.507
	$\eta$ (%)	1.507	0.619	1.096	0.137	1.285
1.00	Call <sub>Model</sub>	16.107	23.444	8.554	16.566	24.555
	Call <sub>MC</sub>	15.944	23.336	8.414	16.585	24.824
	$\eta$ (%)	1.012	0.461	1.637	0.115	1.095
1.05	Call <sub>Model</sub>	18.426	25.527	10.901	18.546	26.290
	Call <sub>MC</sub>	18.129	25.622	10.792	18.829	27.023
	$\eta$ (%)	1.612	0.372	1.000	1.526	2.788
1.10	Call <sub>Model</sub>	20.731	27.553	13.459	20.552	27.998
	Call <sub>MC</sub>	20.572	27.391	13.347	20.630	28.051
	$\eta$ (%)	0.767	0.588	0.832	0.380	0.189
1.15	Call <sub>Model</sub>	23.002	29.517	16.158	22.570	29.677
	Call <sub>MC</sub>	22.865	29.389	16.170	22.716	29.879
	$\eta$ (%)	0.600	0.434	0.074	0.647	0.681

Table 5.4: Call prices generated from model and Monte Carlo simulations for various moneyness levels.

## 5.2 Sensitivity Analysis

In the previous section we observed the change in call prices from our formula with variation in time-to-maturity and moneyness levels. The purpose of this section is to illustrate the sensitivity of call prices from our model with respect to the Heston model parameters in Equation (4.4). We have already justified the accuracy of our model by performing extensive analysis alongside Monte Carlo simulations, and therefore, we will not compare our results to simulations in this section.

The parameter sensitivity analysis procedure follows two steps. First, we illustrate the call price values while varying the parameter within a specific range. Then, to better understand the sensitivity of call prices, we illustrate the rate of change of call prices

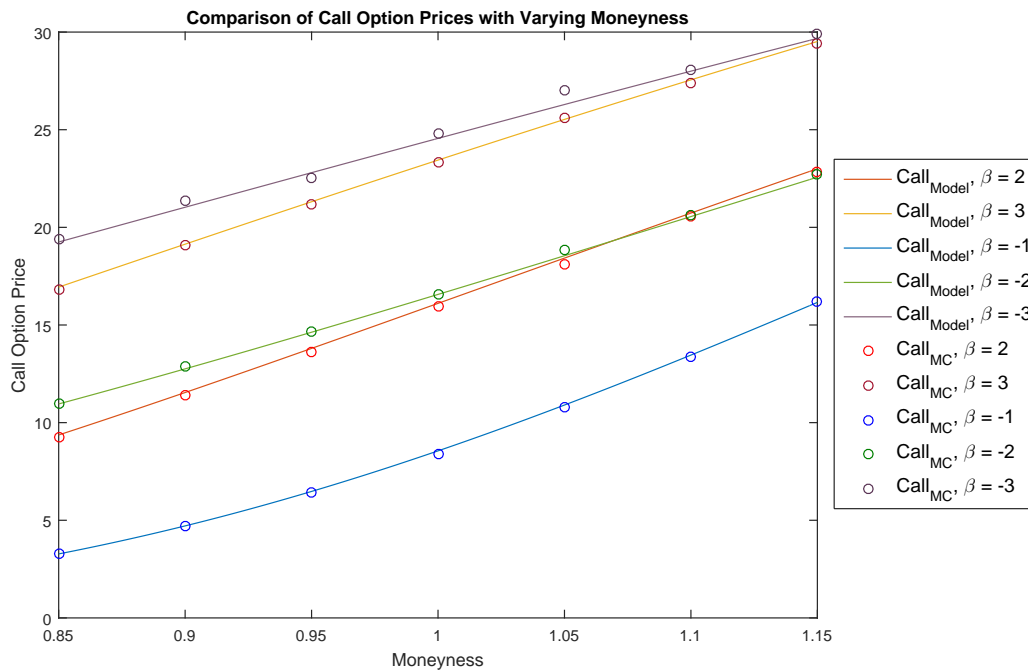


Figure 5.5: Comparison of error between  $\text{Call}_{\text{Model}}$  and  $\text{Call}_{\text{MC}}$  with varying moneyness.

when we vary the parameter. We do this by partitioning the parameter range into 100 discrete, evenly spaced points. We determine the call price at each point, and illustrate the difference in call prices between two adjacent points. Essentially, we calculate the change in call prices with small changes in parameter values. We use a simple change in call prices rather than a percentage change, since the results from the latter are too similar across different  $\beta$  values for some parameters, which makes it difficult to identify behaviour patterns.

### 5.2.1 Long-Run Variance Mean $\theta$

The long-run variance mean,  $\theta$ , is a strictly positive parameter. Also, it is rare for a financial asset to reach a variance greater than 100%. Therefore, we perform sensitivity analysis on  $\theta$  within the range  $[0,1]$ .

Figure 5.6 shows the call price for various values of  $\theta$ . From the figure we can see

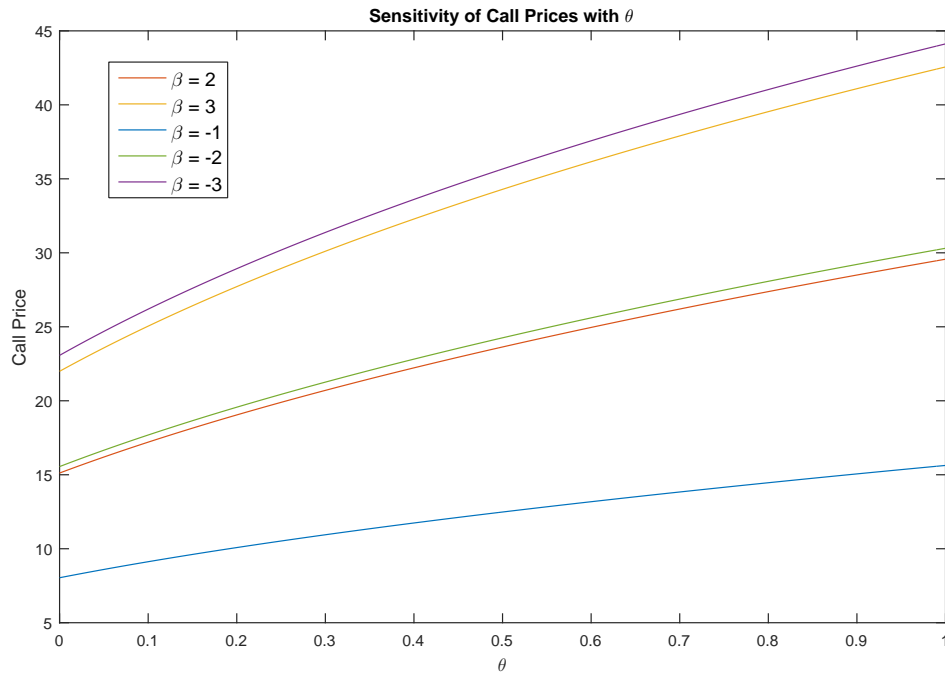


Figure 5.6: Sensitivity of call option prices with  $\theta$ .

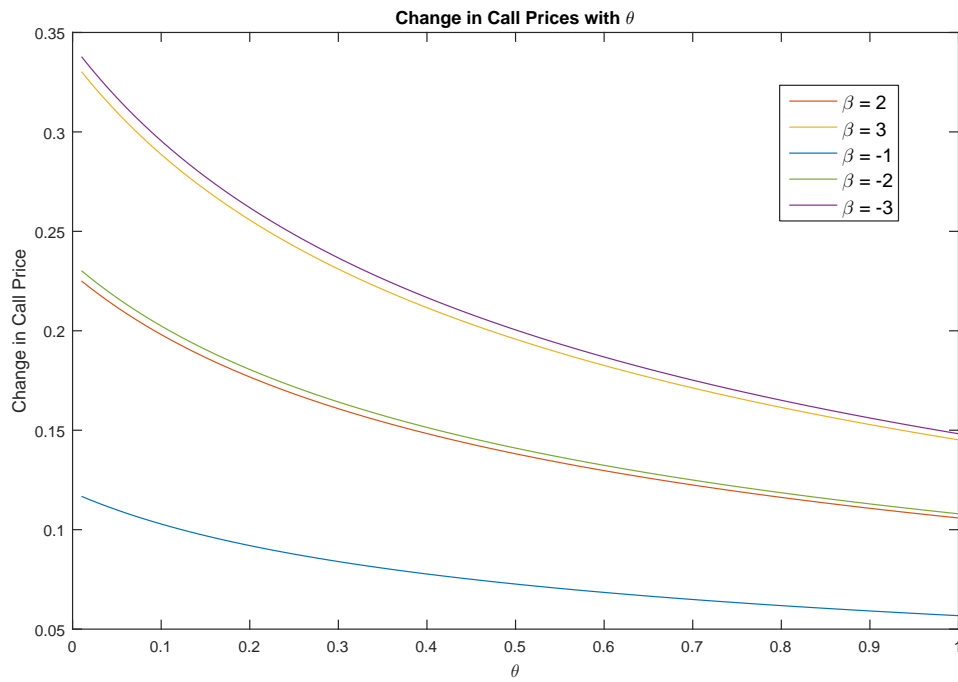
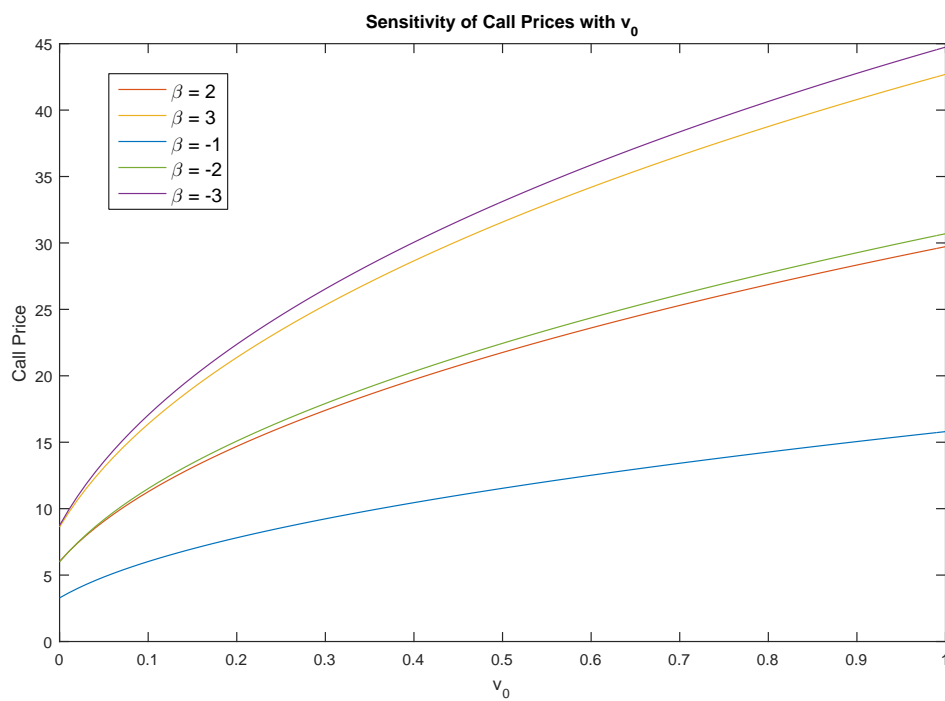
larger absolute  $\beta$  values have a higher call price, as expected. We also observe that bullish LETFs have a lower call price than their bearish counterparts.

Figure 5.7 better illustrates the sensitivity of call prices with  $\theta$ . A positive value for the change in call price indicates that the call price is increasing with  $\theta$ , but the curves themselves have negative slopes which means the call prices are increasing at a decreasing rate. The call prices of LETFs with larger absolute values of  $\beta$  are more sensitive to changes in  $\theta$ , and bearish LETF call prices are more sensitive than bullish LETF call prices.

### 5.2.2 Initial Variance $v_0$

The initial variance  $v_0$ , is similar to  $\theta$  and is also a strictly positive parameter. Therefore, we perform the sensitivity analysis within the range  $[0,1]$ .

Figure 5.8 illustrates the call prices with various values of  $v_0$ . Comparing Figures

Figure 5.7: Rate of change of call option prices with  $\theta$ .Figure 5.8: Sensitivity of call option prices with  $v_0$ .

5.8 and 5.6, we see that the call price reacts similarly to changes in  $\theta$  and  $v_0$ . The call prices are higher for bearish LETFs and also for LETFs with larger absolute  $\beta$  values.

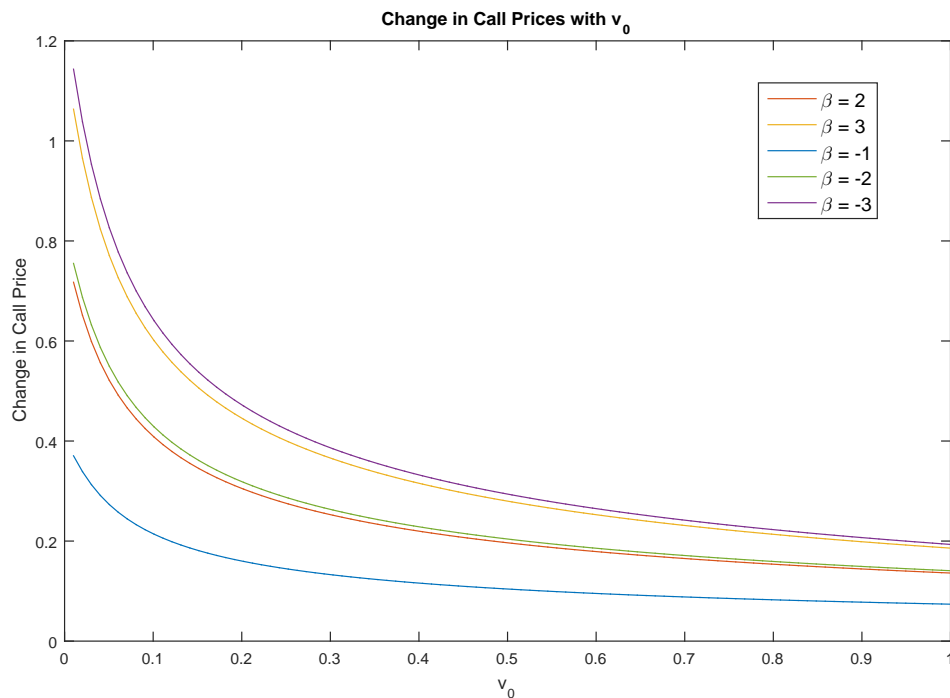


Figure 5.9: Rate of change of call option prices with  $v_0$ .

Figure 5.9 shows the changes in call prices with varying  $v_0$ . Comparing this figure to Figure 5.7, we notice that the call prices are initially more sensitive to changes in  $v_0$  than  $\theta$ . The slopes of the curves in Figure 5.8 are also negative, and therefore, the call prices are increasing at a decreasing rate with changes in  $v_0$ . If we compare the slopes in Figures 5.6 and 5.8, we can tell that Figure 5.8 has much steeper slopes and therefore, the rate of change of call prices is decreasing at a faster rate with  $v_0$ .

### 5.2.3 Variance Mean Reversion Rate $\kappa$

The variance mean reversion rate parameter,  $\kappa$ , is another non-negative parameter. Theoretically,  $\kappa$  can take any positive value but we restrict the parameter to practical values within the range  $[0,10]$ .

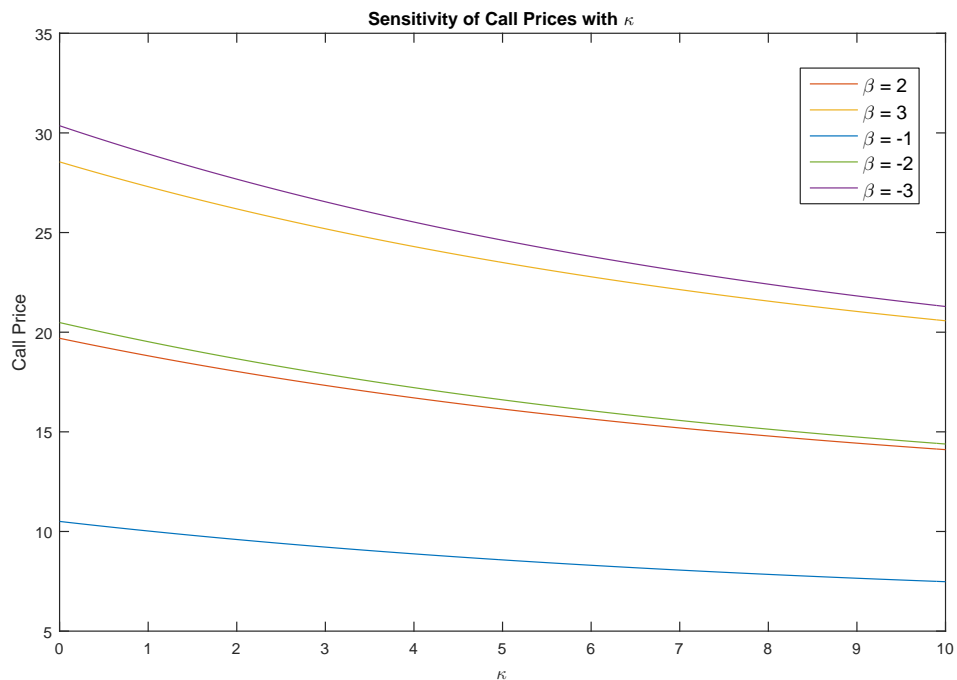


Figure 5.10: Sensitivity of call option prices with  $\kappa$ .

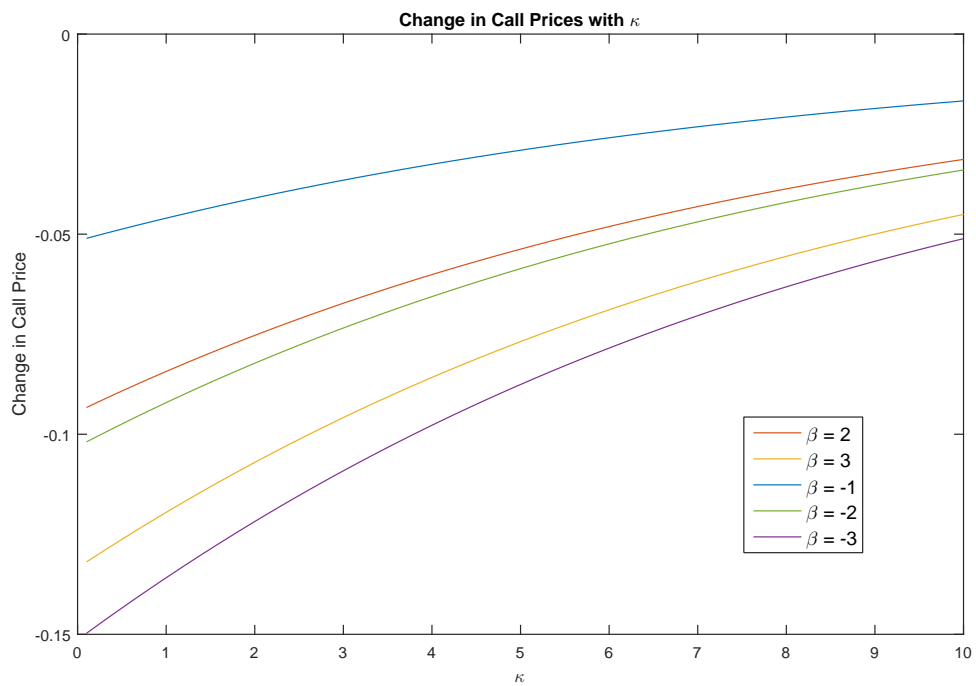
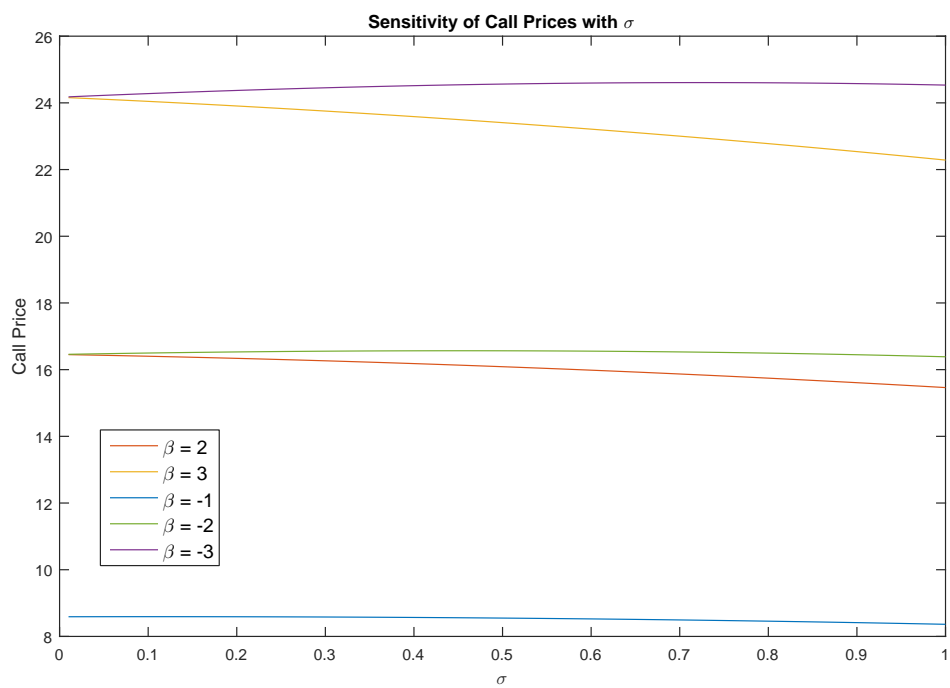
Figure 5.10 shows the ETF call prices with changes in  $\kappa$ . We can see that the call price is higher for bearish ETFs and also for ETFs with larger absolute values of  $\beta$ . Also, the call price decreases with increasing values of  $\kappa$ .

Figure 5.11 illustrates the change in call prices with varying  $\kappa$  values. We can see that the change in call prices is larger for bearish ETFs and ETFs with larger absolute  $\beta$  values. All five curves in Figure 5.11 have upward slopes, and therefore, the call price is decreasing at a decreasing rate for all  $\beta$  values.

#### 5.2.4 Volatility of Variance $\sigma$

We consider the volatility of variance,  $\sigma$ , to be less than or equal 100%. Since  $\sigma$  is also a non-negative parameter, the range for  $\sigma$  is  $[0,1]$ .

Figure 5.12 shows the call prices with changes in  $\sigma$ . Again, we can see the call prices are larger for bearish ETFs and this difference in call prices between bearish and

Figure 5.11: Rate of change of call option prices with  $\kappa$ .Figure 5.12: Sensitivity of call option prices with  $\sigma$ .

bullish LETFs increases for larger values of  $\sigma$ . Interestingly, the call price of bearish LETFs is not very sensitive to changes in  $\sigma$ .

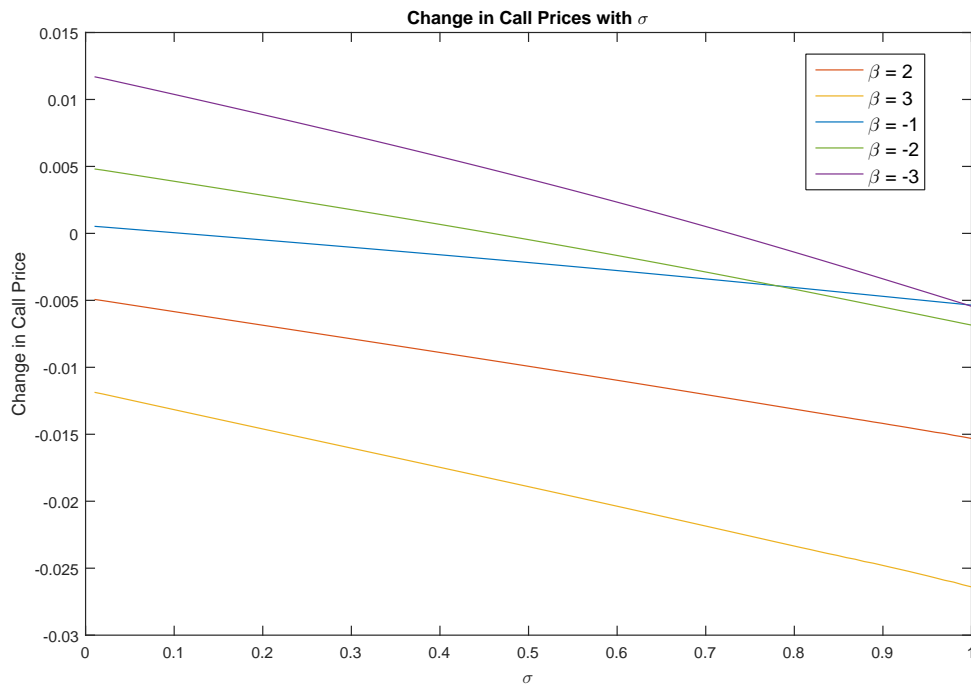


Figure 5.13: Rate of change of call option prices with  $\sigma$ .

Figure 5.13 shows the changes in LETF call prices with varying  $\sigma$ . Immediately we see that the three bearish LETFs are initially increasing as  $\sigma$  is decreasing, but eventually start to decrease. Overall, the bearish LETF call prices are, at first, increasing at a decreasing rate, and eventually, decreasing at an increasing rate, signified by their constant downward slope. The bullish LETF call prices are constantly decreasing at an increasing rate.

### 5.2.5 Stock Price and Variance Correlation $\rho$

The correlation between the stock price and its variance is generally considered to be negative. On many occasions, when the financial market crashes, volatility spikes upwards. However, it may be interesting to visualize a positive correlation and for this

reason we consider the full range of  $\rho$  as  $[-1,1]$ .

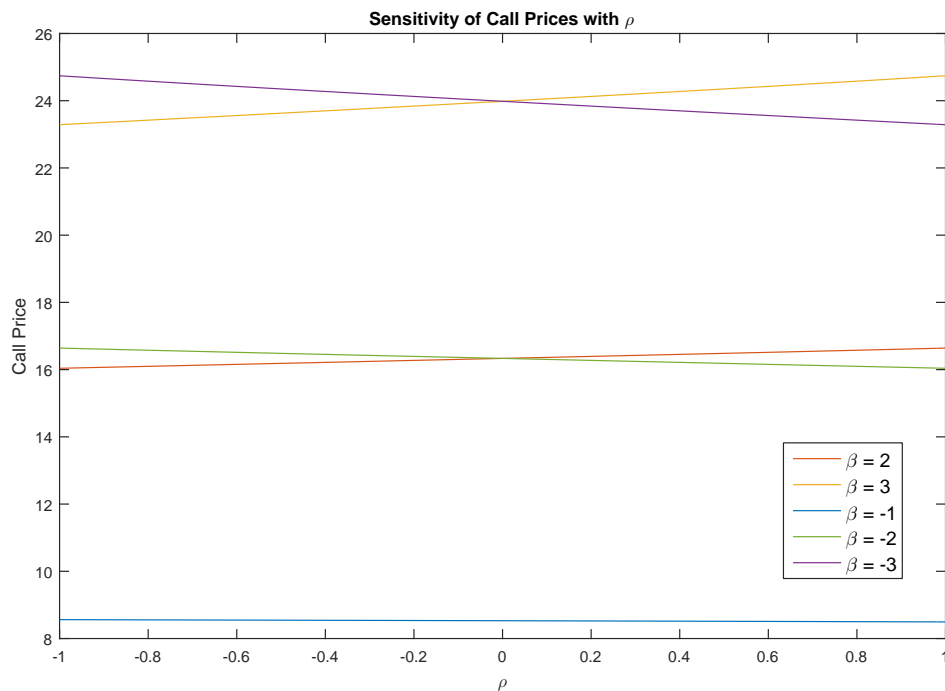


Figure 5.14: Sensitivity of call option prices with  $\rho$ .

Figure 5.14 illustrates the call prices with varying  $\rho$  values. We observe that the call price is relatively less sensitive to changes in  $\rho$  than with other parameters. Interestingly, for  $\rho < 0$ , bearish LETFs have a higher call price than their bullish counterparts. On the other hand, for  $\rho > 0$ , bullish LETFs have a higher call price. We can see that bullish LETF call prices are constantly increasing with increasing  $\rho$  values, and bearish LETF call prices are constantly decreasing.

Figure 5.15 provides an interesting visualization of the change in call prices as  $\rho$  varies. Notice that for LETFs with  $\beta = 2, -1$  and  $2$ , we have an approximately constant rate of change of call prices, with bullish LETF prices having a positive change and bearish LETFs having a negative change in option prices. It is evident from the  $\beta = -3$  curve that bearish LETF prices are decreasing at a slower rate as  $\rho$  increases, especially at lower levels of  $\rho$ . On the other hand, observing the  $\beta = 3$  curve shows that bullish

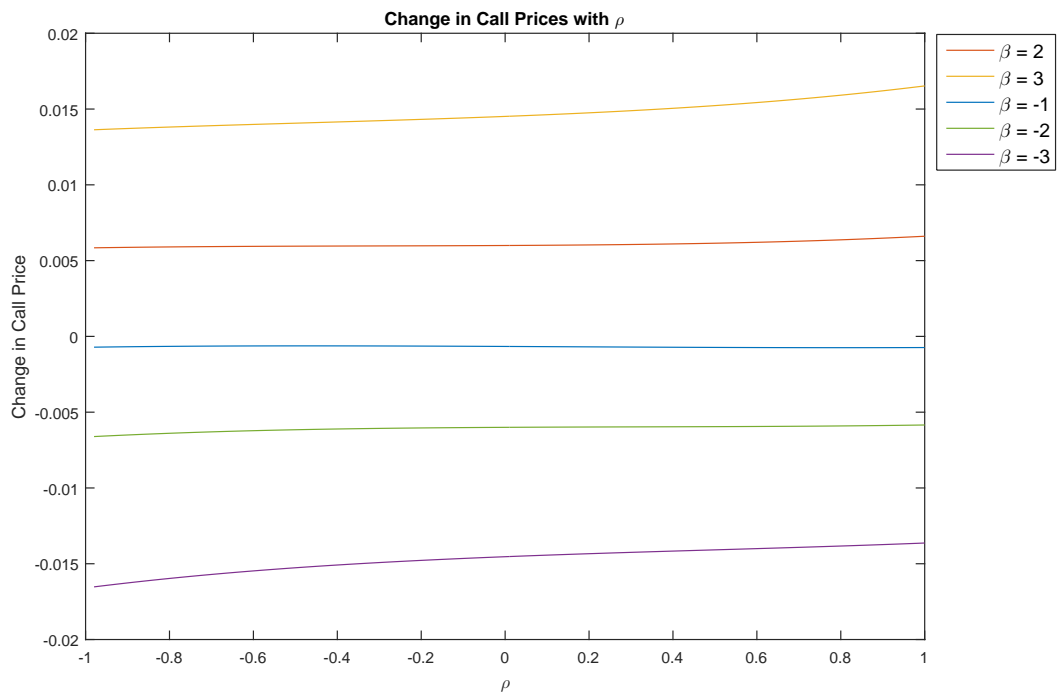


Figure 5.15: Rate of change of call option prices with  $\rho$ .

LETf prices are increasing at a faster rate as  $\rho$  increases, especially for larger  $\rho$  values. From this figure we can state that the change in call option prices is approximately linear with respect to a change in  $\rho$ .

## Chapter 6

### Conclusion and Future Research

Firstly, this thesis introduces a model to link the price of an ETF with its underlying asset. This model is successfully verified by using empirical data of 3 major US equity indices and several of their ETFs as well as two VIX ETFs. The validation of this model consists of determining the variation between the theoretical and empirical ETF prices, and the results show consistently low errors for our chosen ETFs with several different leverage ratios. The justification of this model is of significant importance, since we use this link to define the characteristic function of an ETF and also to obtain Monte Carlo simulations to evaluate call option prices.

We also use an optimization technique [15] as an alternative to linear regression to estimate the empirical leverage ratio values for our ETFs. The drawbacks of using regression are discussed in depth in Chapter 3, but its main disadvantage is its inability to provide a consistent result for the leverage ratio. The results of each method are compared, and the optimization technique provides closer leverage ratio estimates to the advertised leverage ratio values, and considering the other drawbacks of regression, it is justified as a better approach to empirical leverage ratio estimation. We use the optimization method to obtain empirical leverage ratios of ETFs in bullish and bearish markets to better understand their investment potential.

The main purpose of this thesis is to build an option pricing model for an LETF when its underlying asset follows the dynamics of the Heston stochastic volatility model. An additional process is introduced in our model to incorporate the path-dependant variance of LETFs. We use the joint MGF of the log-asset price, its variance and the new path-dependent process to derive a PDE. This PDE is converted into a set of four ODEs, for which we derive a closed-form solution. We then obtain the characteristic function of an LETF using the relationship between LETFs and their underlying asset, which was modeled earlier. We derive a link between the CF and the joint MGF which allows us to use standard transform methods to obtain an option pricing formula. Applying the Carr-Madan formula for option pricing [6], which introduces a dampening factor to make our call price function square-integrable, we are able to derive a suitable call option price formula in the form of an integral.

We numerically solve our call price integral to obtain call prices for specific parameters. To compare our results, we simulate theoretical LETF call prices using an Euler discretization scheme for the Heston model. This process involves using the discretized Heston model to create a time series for the value of the underlying index and its variance. These values then allow us to obtain a time series of LETF prices using the established link between an LETF and its underlying index. We then discount the final LETF price in our time series to time 0, which is essentially the call price of an LETF at time 0. This process is repeated numerous times and averaged to obtain an accurate approximation for the theoretical call price of an LETF. Our option pricing formula compared with Monte Carlo simulations provides reasonably low errors for various  $\beta$ -LETFs.

Finally, sensitivity analysis is conducted to test the performance of our model for different time-to-maturity,  $T$  values, various moneyness levels and with varying model parameters. This analysis is done for leverage ratios ranging from  $-3$  to  $3$  to incorporate all types of LETFs which are popular in the financial market. Our formula provides

results consistent to that of Monte Carlo simulations with varying parameters, and validates the accuracy of our model.

We are able to successfully create an option pricing framework for LETFs which incorporates its path-dependence. A possible extension to our research would be to explore different dynamics for the underlying index. We priced LETF options under Heston stochastic volatility dynamics but it would be interesting to observe results with the addition of jumps in the underlying asset. Using a jump-diffusion process could certainly provide better results for VIX LETF options, since the underlying asset is prone to instability and large movements. Experimenting with different dynamics could provide useful insight for the behavior of LETFs in different financial sectors and lead to more consistent pricing methods. As such, possible future work could involve analyzing LETFs from various financial sectors and optimizing the dynamics of their underlying asset to adapt to the specific characteristics in their relevant sector.

## References

- [1] Ahn, A., Haugh, M., Jain, A. (2015). Consistent pricing of options on leveraged ETFs. *SIAM Journal on Financial Mathematics*, **6**, 559-593.
- [2] Aït-Sahalia, Y., Kimmel, R. (2007). Maximum likelihood estimation of stochastic volatility models. *Journal of Financial Economics*, **83**, 413-452.
- [3] Alexander, C., Kaeck, A. (2010). VIX dynamics with stochastic volatility of volatility. Reading University.
- [4] Avellaneda, M., Zhang, S. (2010). Path-dependence of leveraged ETF returns. *SIAM Journal of Financial Mathematics*, **1**, 586-603.
- [5] Cao, J., Kapoor, G., Ruan, X., Zhang, W. (2018). Path-dependent leveraged exchange-traded fund option valuation using the fast Fourier transform. Submitted to *Computers and Mathematics with Applications*.
- [6] Carr, P., Madan, D. (1999). Option valuation using the fast Fourier transform. *Journal of Computational Finance*, **2**, 61-73.
- [7] Cheng, M., Madhavan, A. (2009). The dynamics of leveraged and inverse exchange-traded funds. *Journal of Investment Management*, **7**, 43-62.
- [8] Cherubini, U., Lunga, G., Mulinacci, S. (2010). *Fourier Transform Methods in Finance*. Wiley Finance.
- [9] Cox, J., Ingersoll, J., Ross, S. (1985). A theory of term structure of interest rates. *Econometrica*, **53**, 385-407.
- [10] Deng, G., Dulaney, T., McCann, C., Yan, M. (2014). Crooked volatility smiles: Evidence from leveraged and inverse ETF options. *Journal of Derivatives and Hedge Funds*, **19**, 278-294.
- [11] Gehricke, S., Zhang, J. (2018). Modelling VXX. *Journal of Futures Market*, forthcoming.
- [12] Guo, K., Leung, T. (2015). Understanding the tracking errors of commodity leveraged ETFs. *Commodities, Energy and Environmental Finance, Fields Institute of Communications*, 39-63.
- [13] Heston, S. (1993). A closed-form solution for options with stochastic volatility with applications to bond and currency options. *Review of Financial Studies*, **6**, 327-343.
- [14] Leung, T., Santoli, M. (2012). Leveraged exchange-traded funds: Admissible leverage and risk horizon. *Journal of Investment Strategies*, **2**, 39-61.
- [15] Leung, T., Santoli, M. (2016). *Leveraged Exchange-Traded Funds: Price Dynamics and Options Valuation*. Springer-Verlag.

- 
- [16] Leung, T., Sircar, R. (2015). Implied volatility of leveraged ETF options. *Applied Mathematical Finance*, **22**, 162-188.
- [17] Lu, L., Wang, J., Zhang, G. (2012). Long-term performance of leveraged ETFs. *Financial Services Review*, **21**, 63-80.
- [18] Mason, C., Omprakash, A., Arouna, B. (2010). Few strategies around leveraged ETFs. *BNP Paribas Equities Derivatives Strategy*, 1-6.
- [19] Øksendal, B. (2003). *Stochastic Differential Equations-An Introduction to Applications*. Springer-Verlag.
- [20] Santoli, M. (2015). *Methods for Pricing Pre-Earning Equity Options and Leveraged ETF Options*. PhD thesis, Columbia University.
- [21] Shreve, S. (2004). *Stochastic Calculus for Finance II: Continuous Time Models*. Springer Science, New York.
- [22] Xu, Y. (2016). *Three Essays on Equity, Volatility and Commodity Derivatives*. PhD thesis, Auckland University of Technology.
- [23] Zhang, J. (2010). *Path-Dependence Properties of Leveraged Exchange-Traded Funds: Compounding, Volatility and Option Pricing*. PhD thesis, New York University.

# Appendix A

## MATLAB Codes

### A.1 LETF Data and Calculating Returns

```
m = length(date);
n = 1000;
ndate = date(m-n+1:m);

% 'database' matrix contains all data. Columns 1, 8, 15, 22 refer
% to underlying indices. Columns 2-7, 9-14, 16-21, 23-25 refer to
% LETFs of the indices from columns 1, 8, 15 and 22, respectively
database = zeros(n,25);
for i = 1:n
    database(i,1:7) = datasnp(m-n+i,1:7);
    database(i,8:14) = datandx(m-n+i,1:7);
    database(i,15:21) = datadji(m-n+i,1:7);
    database(i,22:25) = datavix(m-n+i,1:4);
end

% calculating log-returns
```

```
logreturn = zeros(n,25);
for i = 2:n
    logreturn(i,:) = log(database(i,:))-log(database(i-1,:));
end

% calculating cumulative returns
cumulreturn = logreturn;
for i = 1:n-1
    cumulreturn(i+1,:) = cumulreturn(i,:) + logreturn(i+1,:);
end

% varying holding period
holdlength = 60;
holdreturn = zeros(n,25);
for i = holdlength+1:n
    holdreturn(i,:) = log(database(i,:))-log(database(i-holdlength,:));
end
```

## A.2 Empirical Validation of LETFs

```
% ref_index and letf_index used to reference different columns
% in database
ref_index = 2;
letf_index = 7;
expense_fee = 0.009;
beta = -3;
r = 0.017;

variance = zeros(n,1);
```

```
emp_letfprice = zeros(n,1);
emp_letfprice(1) = database(1,ref_index);
emp_letfreturn = zeros(n,1);

% theoretical LETF price calculation
for i = 2:n
    mean_refreturn = mean(logreturn(1:i,ref_index));
    variance(i) = sum((logreturn(1:i)-mean_refreturn).^2);
    emp_letfprice(i) = exp(log(emp_letfprice(1)) + ...
        beta*log(database(i,ref_index)/database(1,ref_index))+ ...
        ((beta-(beta^2))/2)*variance(i) + ...
        ((1-beta)*r-expense_fee)*(i/n));
    emp_letfreturn(i) = log(emp_letfprice(i)/emp_letfprice(i-1));
end

emp_cumulreturn = zeros(n,1);
for i = 2:n
    emp_cumulreturn(i) = emp_cumulreturn(i-1) + emp_letfreturn(i);
end

% error between theoretical and empirical returns
error = zeros(n,1);
for i = 1:n
    error(i) = exp(logreturn(i,letf_index))-exp(emp_letfreturn(i));
end

error_mean = mean(error);
error_std = std(error);
```

### A.3 Empirical Leverage Ratio Estimation - Optimization Method

```
A = zeros(n,1);
B = zeros(n,1);
C = zeros(n,1);
D = zeros(n,1);

ref_index = 22;
letf_index = 25;
holdperiod = 5;
expense_fee = 0;
dt = holdperiod/252;
variance = zeros(n,1);
meanholdperiod_return = zeros(holdperiod,1);
holdperiod_refreturn = zeros(n,1);
holdperiod_letfreturn = zeros(n,1);

% calculating hoding period return and variance
for i = holdperiod+1:n
    meanholdperiod_return(i) = ...
        mean(logreturn(i-holdperiod+1:i,ref_index));
    variance(i) = ...
        sum((logreturn(i-holdperiod+1:i)-meanholdperiod_return(i)).^2);
    holdperiod_refreturn(i) = ...
        log(database(i,ref_index)/database(i-holdperiod+1,ref_index));
    holdperiod_letfreturn(i) = ...
        log(database(i,letf_index)/database(i-holdperiod+1,letf_index));
    positivereturn = zeros(n,25);
    for j = 1:n
```

```

        if holdperiod_refreturn(j)<0
            positivereturn(j)=holdperiod_refreturn(j);
        else
            positivereturn(j)=0;
        end
    end

    A(i) = -(variance(i)^2)/2;
    B(i) = (3/2)*(holdperiod_refreturn(i)-(r-expense_fee)*dt)*variance(i)...
        + variance(i)^2;
    C(i) = -(holdperiod_refreturn(i)-(r-expense_fee)*dt+(1/2)*variance(i))^2...
        + variance(i)*((r-expense_fee)*dt-holdperiod_letfreturn(i));
    D(i) = (holdperiod_letfreturn(i)-(r-expense_fee)*dt)* ...
        (holdperiod_refreturn(i)-(r-expense_fee)*dt+(1/2)*variance(i));

end

% polynomial coefficients
a = sum(A);
b = sum(B);
c = sum(C);
d = sum(D);

polynomial = [a b c d];
empirical_beta = roots(polynomial)

```

## A.4 Empirical Leverage Ratio Estimation - Regression

### Method

```

regressX = zeros(n-1,3);
regressY = zeros(n-1,1);

```

```
for i = holdperiod+1:n-1
    holdperiod_variance = zeros(holdperiod,1);
    holdperiod_return = mean(logreturn(i-holdperiod:i,ref_index));
    for j = i-holdperiod:i
        holdperiod_variance(j) = (logreturn(j,1)-holdperiod_return)^2;
    end
    regressY(i) = ...
        log(database(i,letf_index)/database(i-holdperiod,letf_index));
    regressX(i,1) = ...
        log(database(i,ref_index)/database(i-holdperiod,ref_index));
    regressX(i,2) = sum(holdperiod_variance);
    regressX(i,3) = 1;
end

regression = regress(regressY,regressX)
```

## A.5 Option Pricing Formula

```
% initializing parameters
L_0 = 100;
S_0 = 100;
moneyness = 1;
K = L_0/moneyness;
alpha = 1.5;
k_0 = log(K);
l_0 = log(L_0);
v_0 = 0.25;
kappa = 5.07;
q = 0;
```

```

theta = 0.0457;
sigma = 0.48;
rho = -0.767;
beta = -3;
r = 0.05;
f = 0.0095;
t = 0;
T = 0.25;
im = sqrt(-1);

% option pricing model
z_1 = @(u) (im*u + alpha + 1)*beta;
z_3 = @(u) (im*u + alpha + 1)*(beta-(beta^2))/2;
delta = @(u) (z_1(u).*rho*sigma-kappa).^2 - ...
    (sigma^2)*(z_1(u).^2-z_1(u)+2.*z_3(u));
lambda1 = @(u) (-(z_1(u).*rho*sigma-kappa)+sqrt(delta(u)))/2;
lambda2 = @(u) (-(z_1(u).*rho*sigma-kappa)-sqrt(delta(u)))/2;
omega = @(u) (exp(lambda2(u).*T).*(-2.*lambda2(u)))/ ...
    (exp(lambda1(u).*T).(2.*lambda1(u)));
A = @(u) (2*kappa*theta/(sigma^2))*log((omega(u).*exp(lambda1(u).*T)+ ...
    exp(lambda2(u).*T))./(omega(u)+1)) + (r-q).*z_1(u).*T;
simcall = @(u) (2/(sigma^2))*((lambda1(u).*omega(u)+lambda2(u))/ ...
    (omega(u) + 1));

final = @(u) (exp((im*u+alpha+1)*(l_0-beta*r*T)- ...
    (im*u+alpha)*(k_0-r*T)+A(u)+simcall(u).*v_0))/ ...
    ((im*u+alpha).(im*u+alpha+1));
hestonCall = (1/pi)*integral(final,0,1000);

hestonCall

```

## A.6 Option Pricing Monte Carlo Simulation

```

N = round(T*252);
m = 1;
N = 10000;
dt = T/N;
beta = 3;

S_m=zeros(N,m);
v_m=zeros(N,m);
L_m = zeros(N,m);
log_return = zeros(N,m);
variance = zeros(N,m);
S_m(1,:)=S_0;
v_m(1,:)=v_0;
L_m(1,:) = L_0;
C = zeros(m,1);

% simulating paths using discretized heston model
for j = 1:m
    for i=2:N
        e1 = normrnd(0,1);
        e2_temp = normrnd(0,1);
        e2 = e1*rho + e2_temp*sqrt(1-(rho^2));
        S_m(i,j) = S_m(i-1,j) + r*S_m(i-1,j)*dt+ ...
            sqrt(max(v_m(i-1,j),0))*sqrt(dt)*S_m(i-1,j)*e1;
        v_m(i,j) = v_m(i-1,j)+kappa*(theta-max(v_m(i-1,j),0))* ...
            dt+sigma*sqrt(max(v_m(i-1,j),0))*sqrt(dt)*e2;
        log_return(i,j) = log(S_m(i,j)/S_m(i-1,j));
        variance(i,j) = sum((log_return(1:i-1,j)- ...
            mean(log_return(1:i,j))).^2);
    end
end

```

```
L_m(i, j) = exp(log(L_m(1, j)) + beta*log(S_m(i, j)/S_m(1, j)) + ...
    ((beta-(beta^2))/2)*variance(i, j) + ((1-beta)*r-f)*i*dt);
end
% theoretical call price
C(j) = exp(-r*T)*max(L_m(N, j)-K, 0);
end

mc_call = mean(C);
mc_call
```